

NO-0189 827

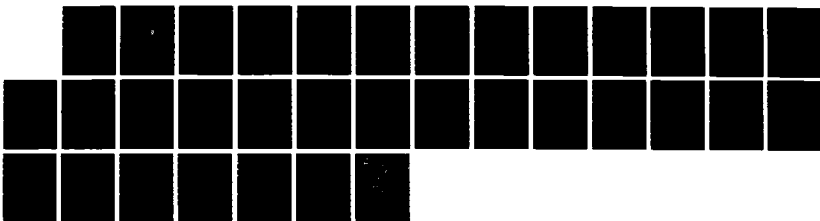
THE PHYSICAL OCEANOGRAPHY OF THE ALBORAN SEA(U) NAVAL  
OCEAN RESEARCH AND DEVELOPMENT ACTIVITY NSTL STATION NS  
G PARRILLA ET AL. MAR 87 NORDA-184

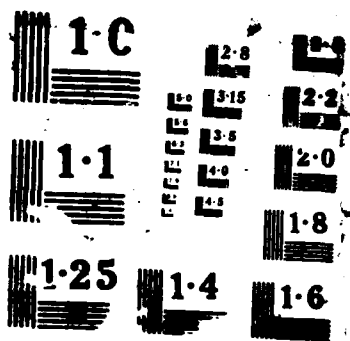
1/2

UNCLASSIFIED

F/G 8/3

NL





# Naval Ocean Research and Development Activity

March 1987

Report 184

DTIC FILE COPY



## The Physical Oceanography of the Alboran Sea

AD-A189 027

DTIC  
ELECTE  
JAN 28 1988  
S D

**Gregorio Parrilla**  
Instituto Español de Oceanografía  
Madrid, Spain

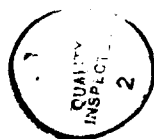
**Thomas H. Kinder**  
Oceanography Division  
Ocean Science Directorate

**ERRATUM** for NORDA Report 184 by Parrilla and Kinder

1. Executive Summary, p. i, line 4: change "36" to "36.5".
2. P. 1, 2nd column, 2nd paragraph, line 12: change "Charnok" to "Charnock".
3. P. 8, Figure legend. Change "10" to "11".
4. P. 11, Figure legends:  
15(d). Change legend to read "Salinity minimum during Cornide de Saavedra cruise in October 1981".  
15(e). Change legend to read "Salinity at 100 m depth during Cornide de Saavedra cruise in October 1981."
5. p. 16, 4th paragraph, line 7: Change "31" to "3".
6. P. 19, 2nd column 2nd paragraph, line 11: Change "3'0" to "30'".
7. P. 23, bottom, last sentence: Change "La Violette, P. E. (1985)" to "La Violette, P. E. (1984)".
8. References, P. 24: Change "primaveraverano" to "primavera-verano".

## Executive summary

The Alboran Sea is the westernmost basin of the Mediterranean Sea. Research published through 1983 is synthesized to show the important physical oceanographic features of the Alboran Sea. The upper layer of the Alboran Sea extends to about 200 m depth, and is characterized by low salinity (36.5 or less) and by an energetic anticyclonic gyre, whose speeds may exceed 1 m/sec and which may fill most of the western Alboran. Beneath the generally eastward-flowing Atlantic Water are two Mediterranean waters. The Levantine Intermediate Water, which extends from about 200 to 600 m depth, has maxima in both salinity (about 38.45) and temperature. The Levantine Water moves westward at 1-3 cm/sec in a broad flow that is concentrated in the northern part of the basin. Below the Levantine Water the Western Mediterranean Deep Water has steadily decreasing salinity and temperature to values below 12.9°C potential temperature, which has been taken as a definition. The deep-water flow is concentrated as a narrow boundary current against the African slope and has a speed of 5-10 cm/sec to the west.



Accession For	
NTIS	CRA&I <input checked="" type="checkbox"/>
ERIC	TAB <input type="checkbox"/>
Unannounced <input type="checkbox"/>	
Justification	
By	
Distribution	
Availability Codes	
Dist	Avail and/or special
A-1	

# Acknowledgments

---

We wish to thank many colleagues who have helped us to study the Alboran Sea. We especially thank those who put in long hours at sea collecting the data on which our knowledge is based. We also wish to express our appreciation to Mr. Angel Esteban, who prepared the illustrations, and to Ms. Joyce Ford, who prepared the original manuscript.

G. Parrilla thanks A. R. Miller for his continuous support during the Alboran Sea studies. Mr. Parrilla was partially funded by the Cooperative Program 3044 sponsored by the Spain—U.S.A. Treaty of Friendship and Cooperation.

T. Kinder was funded by the Coastal Sciences Section of the U.S. Office of Naval Research. The work was supported by Program Element 61153N, Dr. Dennis Conlon and Dr. Alan Brandt, Program Managers.

# Contents

---

<b>I. Introduction</b>	<b>1</b>
<b>II. Physiography</b>	<b>1</b>
<b>III. General meteorological conditions</b>	<b>3</b>
A. Prevailing winds	3
1. Ponientes	3
2. Levantes	3
3. Terrales	3
4. Southerly and southwesterly winds	4
<b>IV. Water masses and their distributions</b>	<b>4</b>
A. Vertical distribution of potential temperature and salinity	4
B. $\theta$ -S correlation	7
C. Atlantic water: the anticyclonic gyre and its variability	7
1. The geographic distribution of Atlantic Water	7
2. The anticyclonic gyre and its variability	12
D. The temperature minimum layer	14
E. The Levantine Intermediate Water	15
F. The Deep Water	17
<b>V. General circulation</b>	<b>19</b>
A. Atlantic Water circulation	19
B. Mediterranean Water circulation	21
<b>VI. Tides and internal waves</b>	<b>21</b>
<b>VII. Meteorological effects on the flow</b>	<b>21</b>
<b>VIII. The future</b>	<b>22</b>
<b>IX. Summary</b>	<b>23</b>
<b>X. An update on related publications</b>	<b>23</b>
<b>XI. References</b>	<b>24</b>

# The Physical Oceanography of the Alboran Sea

## I. Introduction

The Alboran Sea has been called the Alboran Channel, which is an apt name for this elongated, semi-enclosed body of water that connects the Strait of Gibraltar to the Western Mediterranean Sea. In a broad sense, the Alboran Sea can be considered a strait, as it is a narrow transition between the broad Mediterranean Sea and the open Atlantic Ocean. Oceanographic phenomena that are regionally interesting or that display interesting ocean physics occur there—in many cases because of the proximity to Gibraltar and because the Alboran serves as a conduit connecting the Atlantic to the rest of the Mediterranean.

Lacombe and Tchernia (1972) described the Mediterranean as a series of basins and sills, and the Western Alboran Sea is the first basin encountered by the inflowing Atlantic Water, and is the last basin occupied by the outflowing Mediterranean Water. These two water types demonstrate their maximum contrast in the Alboran. The less saline Atlantic Water emerges from the Strait of Gibraltar as a narrow and energetic current (speeds  $>1$  m/sec), and then forms a permanent anticyclonic gyre in the western Alboran that nearly extends from Spain to Morocco. The Mediterranean Water enters the Alboran from the east as a more diffuse and unenergetic (speeds  $\sim 0.01$  m/sec) flow. The intermediate water shows a preference for the northern half of the sea, but the deep water forms an identifiable current that adheres to the African slope before flowing upward toward the sill at Gibraltar. Both intermediate and deep water contribute to the outflow into the Atlantic. The exchange of waters through the Strait of Gibraltar is closely related to budgets of water, salt, heat, nutrients, and pollutants for the entire Mediterranean. The structure and behavior of water masses and flows in the Alboran Sea provide clues to the fluxes that comprise these exchanges and to the exchange processes themselves.

The best summary of the Alboran was produced by Lanoix (1974). Although he relied on data from the summer of one year (1962), his analysis was thorough and comprehensive. Other helpful reviews that included the Alboran were Lacombe and Tchernia (1972) and Hopkins (1978). These reviews covered the entire

Mediterranean and the western Mediterranean, respectively, but they were especially useful for placing the Alboran Sea in broader perspective.

This material was given as a paper at the NATO Advanced Research Workshop on the Oceanography and Meteorology of the Mediterranean Sea (Santa Teresa, La Spezia, Italy; September 1983). Although nearly four years have passed since this manuscript was written, our overview is useful because it synthesizes knowledge of the Alboran Sea and reports on some data that are either unpublished or appear only in obscure reports. A volume on the Mediterranean Sea for which this report was originally written should appear soon (*The Oceanography and Meteorology of the Mediterranean Sea*, H. Charnock ed., in prep.). The volume will include many review papers that describe various regions within the Mediterranean, and it will offer a more complete picture of the physical oceanography of the Mediterranean Sea than is presently available.

This material is being issued as a report to ensure a wider distribution than afforded by the book alone. A Spanish version is being issued simultaneously by the Instituto Español de Oceanografía in Madrid.

This report is organized as follows. First we present an overview of the physiography (II) and meteorology (III) as necessary background to the next two sections. The core of the paper is contained in the sections on water masses (IV) and general circulation (V). These sections overlap somewhat because it is impossible to make sense of one topic without a knowledge of the other. The general circulation uses results of direct current measurements, of which there have been many in the past 8 years (but few results have been published). We then have two short sections on specialized topics that have received strong interest: tides and internal waves (VI) and meteorological effects on the flow (VII). We conclude with a comment on the immediate future of research in the Alboran (VIII), a brief summary (IX), an update on recent related publications (X), and the references (XI).

## II. Physiography

The physiography of the Alboran Sea has a profound influence on the distribution of water masses



and on the circulation, as sections IV and V will show. We therefore review the major features that constrain the flow of both Atlantic and Mediterranean waters. This discussion closely follows J. P. Flanagan in Carter et al. (1972) and is also based on U.S. Defense Mapping Agency Chart 52000. We have used some of the nomenclature of Milliman et al. (1972) and of Huang and Stanley (1972).

The Alboran Sea is located in the westernmost Mediterranean Sea and forms a narrow (100 km) approach to the Strait of Gibraltar (Fig. 1). It is bordered on the north by Spain, on the south by Morocco and western Algeria, on the west by the Strait of Gibraltar, and on the east by the line joining Cabo de Gata (Spain) and Cabo Figalo (Algeria) (as defined by the International Hydrographic Organization). The Alboran Sea is connected to the North Atlantic Ocean through the narrow (15 km) and shallow (300 m) Strait of Gibraltar and is open at its eastern boundary to the western Mediterranean. It has an area of 54,000 km<sup>2</sup>, and a maximum depth of nearly 1500 m in the western basin and about 2000 m at its eastern limit.

The bottom topography of this small sea is complex. The width of the continental shelf (called "upper shelf" by Flanagan) varies from 2 to 10 km off the Spanish Coast. It is wide (10 km) off Malaga and narrow (2 km) off Cape Sacratif, and averages about 5 km in width. Along the African Coast the shelf is 3 km wide from Punta Almira to Point Busicur, then it fluctuates from 3 to 18 km width to Cabo Tres Forcas, and then it is a uniform 15 km width eastward. The depth of the shelf break varies from 100 to 150 m.

Seaward of the shelf break is a region of varied physiographic features. This region is especially prominent along the African Coast and was called the "lower shelf" by Flanagan. Two elongated and gently sloping plateaus cover much of this region between Punta Almira and Xauen Bank (92 km x 27 km) and between

Cabo Tres Forcas and Cape Figalo (135 km x 63 km). A third large (80 km x 55 km) plateau is found near the Spanish Coast between 3° and 4° W. This plateau, which contains several volcanic peaks, has a lower boundary delineated by the 900 m isobath. A steep continental slope that leads to the Alboran Strait (Giermann, 1962) has depths near 1500 m and connects the western Alboran Basin to the Algerian Basin. There is no sill in the eastern Alboran as was implied by Wust (1961; see Katz, 1972).

There are also a number of ridges, valleys, and banks. Xauen and Tofino banks come within 100 m of the surface near the Moroccan Coast at 4°W, and Provencaux, Cabliers, and Alidade Banks are found in the southern half of the eastern Alboran. Djibouti Bank rises within 200 m of the surface northwest of Alboran Strait. Between Xauen Bank and Cabo Tres Forcas is a long (160 km) northeast/southwest-oriented ridge ("Seuil d'Alboran," Giermann et al. 1968) that contains Xauen and Tofino Banks, as well as Alboran Island. The ridge is separated from Africa by a narrow trough ("South Alboran Graben," Giermann, 1962) whose sill depth is deeper than 400 m.

The Eastern and Western Alboran are separated near 3°W by Cabo Tres Forcas, Alboran Island, and the restrictions in the troughs north and south of Alboran Island (Alboran Strait and South Alboran Graben). Each half of the Alboran Sea contains a basin (in the geological sense, the deep parts of each half are often called "basins"). The Western Basin is defined by the 1400-m contour and is elongated in the east-west direction. It is 40 km x 22 km, reaches a maximum depth in excess of 1500 m, and is connected to the Alboran Strait. The eastern Alboran Basin is smaller, only 13 km x 6 km, and is defined by the 1200-m contour. It is located southwest of Alboran Island and is connected to the Algerian Basin to the east by the southern trough (South Alboran Graben). The eastern Alboran is dominated by a broad depression that opens eastward into the Algerian Basin.

Alboran Island is a small (600 m x 250 m) volcanic island that sits atop the long ridge (Seuil d'Alboran). The island is surrounded by a shallow (less than 200 m depth), flat-topped plateau that extends 45 km northeast-southwest and has a maximum width of 10 km. Depths on both sides of the plateau drop off steeply into Alboran Strait to the north and into the trough leading to the East Alboran Basin on the south.

In summary, the periphery of the Alboran Sea has a narrow continental shelf with widths less than 20 km and usually less than 10 km. The continental slope is interrupted by plateaus and banks of varying sizes and depths. The western Alboran, where depths extend to 1500 m, is connected to the east by a deep channel north of the ridge that is topped by Alboran Island and by a shallower trough south of this ridge. The Eastern Alboran is open to the deeper and larger Algerian Basin to the east.

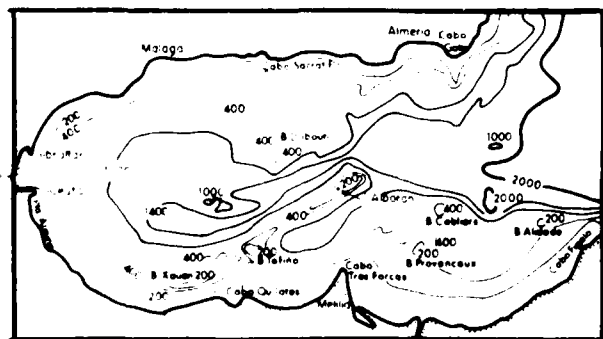


Figure 1. Bathymetry of the Alboran Sea in meters. Redrawn from chart 310 published by the Defense Mapping Agency Hydrographic Center, Washington, D.C.

### III. General meteorological conditions

Forcing by the atmosphere influences water mass transformation and affects the circulation (Section VII). We discuss both the large-scale meteorology and the local wind systems. This discussion is based on Brody and Nestor (1980), Admetlla (1980), and Anonymous (1982).

The seasonal weather pattern in the Alboran Sea is strongly influenced by the movement of the semipermanent Azores anticyclone. During winter (November–February), the anticyclone diminishes as the upper-level westerlies and associated storm tracks move southward. Migrating cyclones and anticyclones cause the weather to be unsettled, wet, and windy. During summer (June–September) the Azores anticyclone extends northeastward toward the Alps, causing warm and dry weather with light winds. The transitional seasons of spring and autumn have different lengths. Spring extends from March through May, and is characterized by an alternation of stormy winter weather and calm summer weather. Autumn lasts only during October, and the transition to winter weather is abrupt.

The mountains that line both the northern and southern shores affect the winds most strongly in the Strait of Gibraltar and near shore and, to a lesser extent, offshore. The mountains increase speed and constrain direction by channeling the winds. They are also conducive to producing such local phenomena as mountain gap winds and katabatic winds.

#### A. Prevailing winds

**1. Ponientes (westerly winds).** These westerly winds are humid and mild, and are associated with low pressure north or northwest of the Iberian Peninsula (Fig. 2). The skies are generally clear with some cumulus clouds, although there may be some showers. This pattern is common during winter and spring. During winter these conditions produce terrales (see following discussion) in the Malaga region. Usually poniente winds last about one week, although occasionally they may last longer. Along the Spanish Coast poniente winds produce a noticeable cooling of the sea surface, probably as a result of upwelling between Estepona and Malaga (terrals can add to this effect).

**2. Levantes (easterly winds).** These winds blow from the east and the southeast, and are associated with high pressure north of the peninsula (Fig. 3). A high-pressure cell over the Balearic Islands can also cause a levante that is localized in the Alboran Sea and the Strait of Gibraltar, sometimes with gale-force winds. Levantes occur in every season. During summer they are associated with the Azores anticyclone that extends over Spain. Weather is usually good, although the warm air moving over the cooler water produces fog and low stratus near Gibraltar. During other seasons levantes are usually associated with cyclonic activity over the western Mediterranean, over Northwest Africa, or over the North Atlantic west of northern

Morocco. These levantes are accompanied by low clouds and frequently by heavy rains.

**3. Terral (from land).** Terrales are two types of northerly winds. The winter terral is associated with high pressure centered near the Alboran (Fig. 4), which

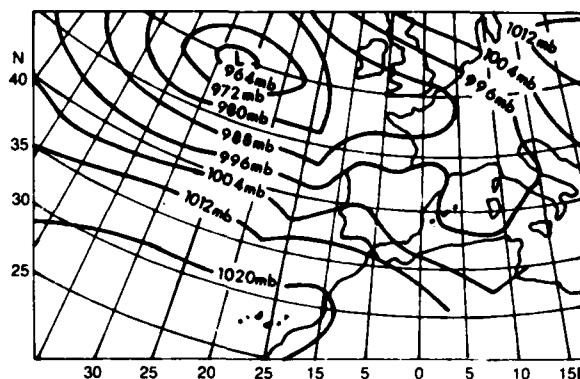


Figure 2. The isobaric chart for poniente winds.

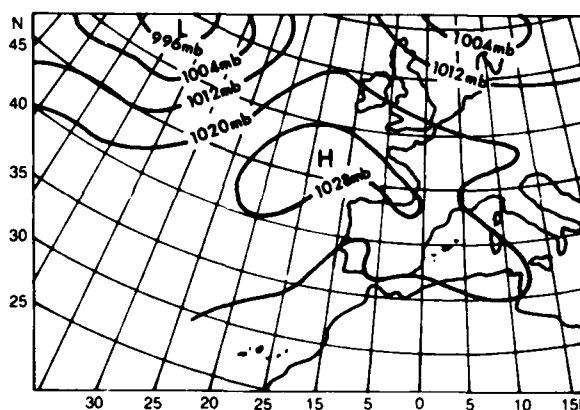


Figure 3. The isobaric chart for levante winds.

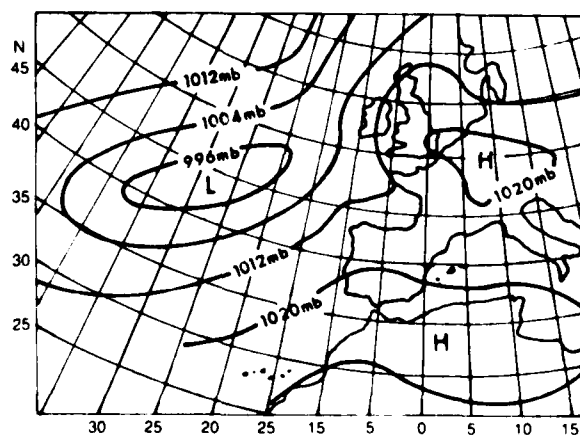


Figure 4. The isobaric chart for katabatic winter terral winds.

generates winds that are channelized by the coastal mountains. These winds are steady and can have speeds up to 15 m/sec. A stronger (winds can reach 25 m/sec) and colder terral occurs when an anticyclone and a cyclone are stabilized in the Atlantic and Mediterranean (Fig. 5). The warm terral of summer is caused by either a high-pressure cell west of the peninsula with a northwest-southeast axis (Fig. 6) or a high-pressure cell between the Azores and Portugal, which causes the westerly wind to turn northwesterly or northerly.

**4. Southerly and southwesterly winds.** These winds are infrequent and are usually associated with low pressures centered in the Gulf of Cadiz (Fig. 7). Skies are cloudy and heavy rains occur along the Spanish Coast. Temperatures are warm and the air sometimes carries reddish dust from the desert in suspension. Near the African coast these winds occur on the average of four to five times per month, mostly during late spring and early summer.

Coastal stations around the Alboran also show a marked land breeze at night and a sea breeze during the day. At Ceuta and Tarifa near the Strait climatological data do not show a strong land-sea breeze, but sea breezes occur at Gibraltar during summer.

The cyclonic activity that affects the region usually originates either west of Gibraltar or in North Africa south of the Atlas Mountains (Fig. 8). Cyclones approaching the Strait of Gibraltar generally move southeastward into North Africa, where they may regenerate south of the Atlas Mountains. Approximately one-third of the cyclones that approach the Strait redevelop over the Alboran Sea and then move eastward into the Western Mediterranean.

May (1982) has constructed wind stress maps based on ship reports for the entire Mediterranean (Fig. 9). His maps show westerly (toward the east) wind stress over the entire Alboran during all four seasons, whereas the wind stress in the Strait and just west of the Strait is easterly (toward the west). The mean annual wind stress magnitude is slightly less than 1 dyne/cm<sup>2</sup>. Table 1 gives some values for meteorological parameters from four stations around the Alboran Coast, and Figure 10 shows monthly air temperatures from a station on Alboran Island.

## IV. Water masses and their distributions

### A. Vertical distribution of potential temperature and salinity

Profiles of potential temperature ( $\theta$ ) and salinity ( $S$ ) (Fig. 11) show the vertical distribution of water masses. The three major water masses are Atlantic Water (AW), Levantine Intermediate Water (LIW), and Deep Water (DW).

AW occupies the upper, nearly isohaline layer. Its thickness varies, ranging from 150 m in the central

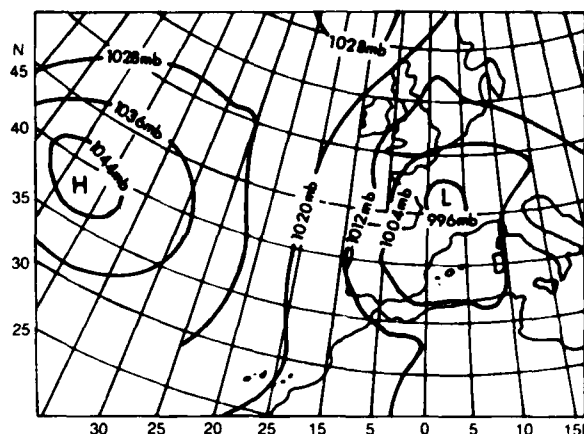


Figure 5. The isobaric chart for cold winter terral winds.

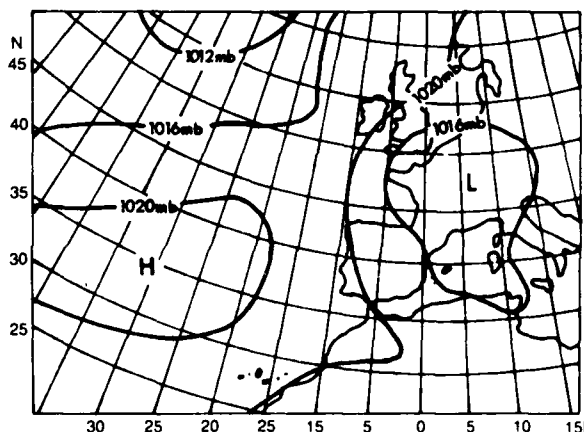


Figure 6. The isobaric chart for summer terral winds.

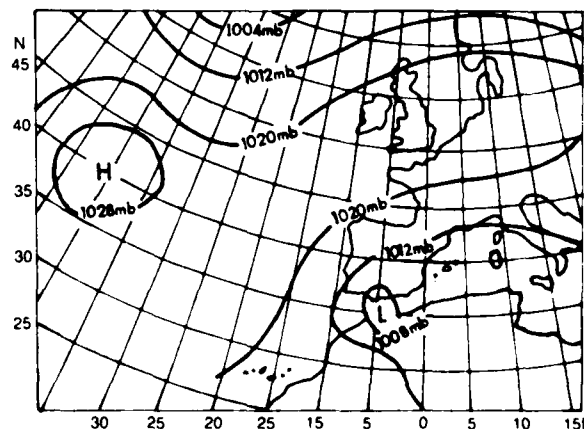


Figure 7. The isobaric chart for southerly winds.

Table 1. Mean values for the period 1931-1960 from Instituto Nacional de Meteorologia, 1982

	Alt	$T_m$	$T_n$	$R_m$	H	I	
Malaga	12	22.8	13.6	500	69	3203	Alt. — Altitude (m)
Almeria	18	21.6	14.3	203	73	3052	$T_m$ — mean air temperature max in °C.
Ceuta	200	19.7	13.8	1200	77	2606	$T_n$ — mean air temperature min in °C.
Melilla	47	23.1	12.8	469	76	2613	$R_m$ — annual precipitation max in mm
							H — annual mean relative humidity
							I — annual mean of sunlight in hours
							Rivers runoff — 120 m <sup>3</sup> /sec = 3.8 km <sup>3</sup> /year (United Nations Environmental Program, 1979)

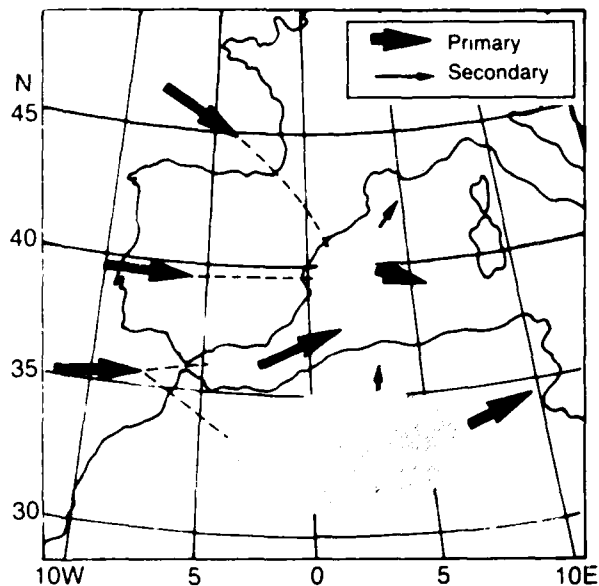


Figure 8. Areas of cyclogenesis and cyclone tracks that affect Gibraltar and the western Mediterranean (from Brody and Nestor, 1980).

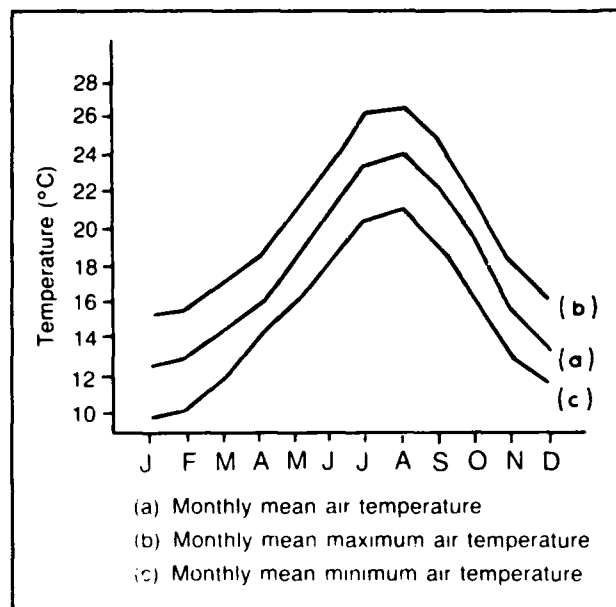


Figure 10. Air temperatures measured at Alboran Island over a two-year period.

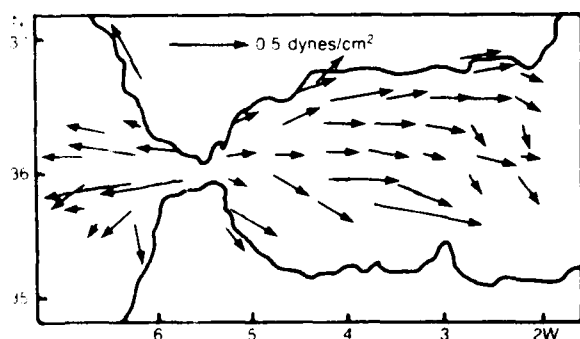


Figure 9. Average wind stress for the period 1947-1973 (courtesy of P. W. May, NORDA).

Western Alboran Basin to less than 50 m near the Spanish Coast. Salinity varies from 36.2 to 36.5 ppt (‰). Throughout most of the Alboran Sea a subsurface salinity minimum exists and is most conspicuous during summer. This layer, found between 10 m and 100 m depth, is generated by surface evaporation above and by more saline Mediterranean waters below. The vertical temperature gradient in the AW changes during the year. In summer the combined seasonal and permanent thermoclines have large gradients (0.04°C/m) from near the surface to as deep as 150 m (the thermocline extends deeper where the AW is thicker). A more detailed  $\theta$  profile (Fig. 11, inset) shows a multiple-step thermocline that is composed of several relatively homogeneous layers with 10 to 20 m thickness and is separated by intense thermoclines ( $> 0.15^\circ\text{C}/\text{m}$ ). Such small-scale features appear at many stations. Statically stable inversions of  $\theta$  with thicknesses of a few meters to tens of meters indicate intrusions of slightly different

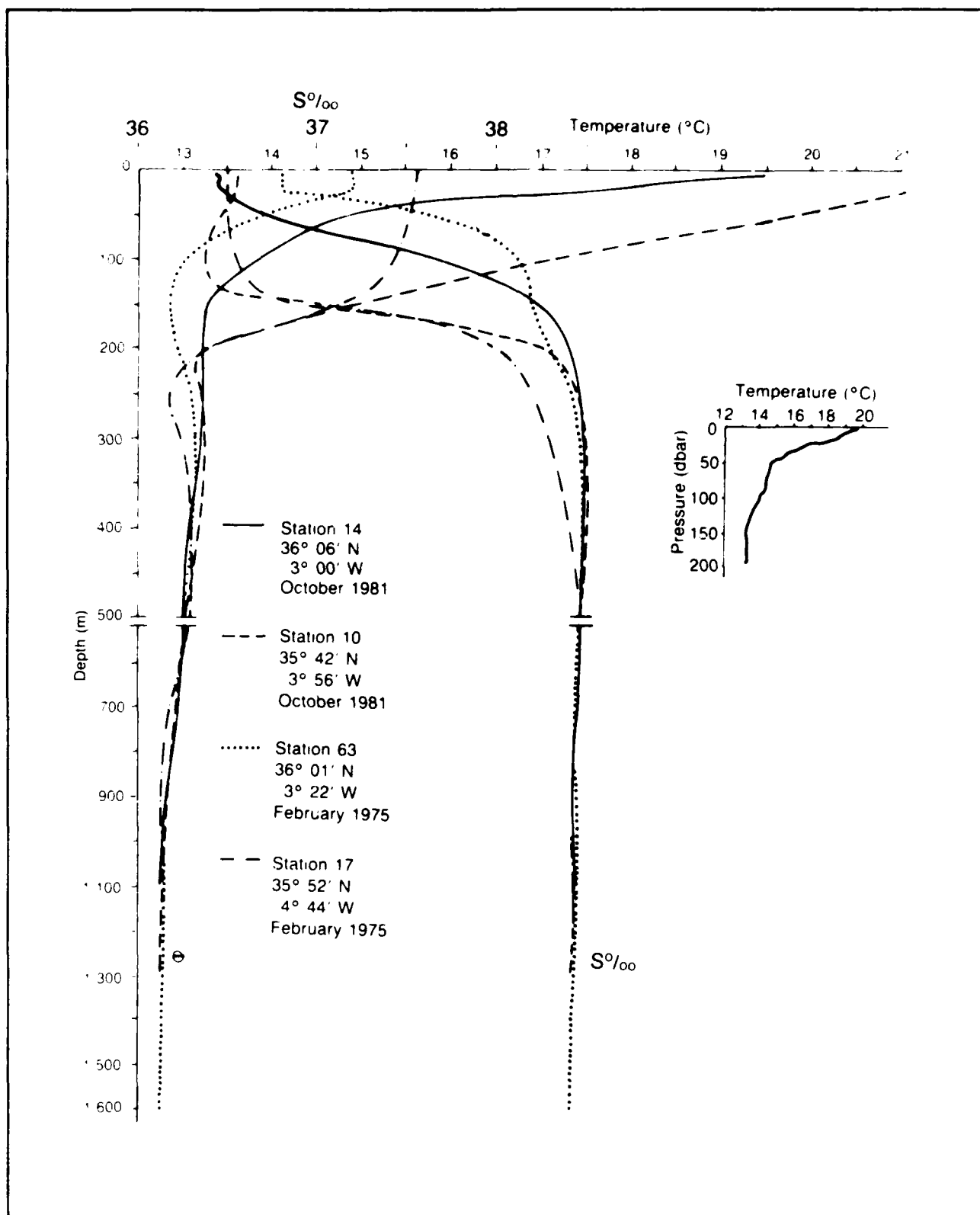


Figure 11. Potential temperature and salinity versus depth for stations 17 and 63 from the R/V Chain (February 1975) and stations 10 and 14 Cornide de Saavedra (October 1981).

waters. A second typical feature is a step structure in  $S$  above the maximum. In winter the AW layer is nearly isothermal and temperature profiles form nearly mirror images of salinity profiles (Fig. 11). Beneath the AW is a transition zone that separates Atlantic and Mediterranean Waters (LIW and DW). The  $\theta$  and  $S$  gradients are strong ( $0.02^\circ\text{C}/\text{m}$ ,  $0.02$  ppt/m) and the transition zone is typically 100 m thick.

Beneath this transition the gradients of  $\theta$  and  $S$  become small. Between 200 and 600 m depth maxima of  $\theta$  and  $S$  are found ( $13.2^\circ\text{C}$ ,  $38.45$ – $38.50$  ppt), indicating the influence of LIW. The  $\theta$  maximum is generally above the  $S$  maximum; multiple maxima are sometimes found at different depths, especially beneath the front near the Strait of Gibraltar. When several  $\theta$  maxima exist, one of them usually coincides with the  $S$  maximum. Below these maxima both  $\theta$  and  $S$  slowly decrease. This is the DW layer, which characteristically has  $\theta < 12.9^\circ\text{C}$  and  $S < 38.44$  ppt. These  $\theta$ - $S$  values are similar to those of deep water formed in the northern part of the Algero-Provençal (Algerian) Basin (so-called MEDOC region) in winter.

A minor water mass is also defined by a  $\theta$  minimum and is often found near 200 m above the LIW. Lanoix (1974) and Cano (1977) believe this water mass has an origin close to the DW formation region, but that it is less dense than DW and sinks only to about 200 m. This water mass was clearly present in 1962 (Lanoix, 1974) and in 1975 (Bryden et al., 1978), but in the data that we gathered recently (1978–1982) the  $\theta$  minimum is very weak and appears more as an inflection of the  $\theta$ - $S$  curve than as a clear minimum.

## B. $\theta$ - $S$ correlation

Figure 12 shows the  $\theta$ - $S$  diagrams for the same stations whose vertical profiles were shown in Figure 11. At station 10 during late summer (October)  $S$  remained nearly constant through 125 m of AW as  $\theta$  decreased from nearly  $22^\circ\text{C}$  to  $16^\circ\text{C}$ .  $S$  remained close to 36.5 ppt with a minimum ( $\sim 36.4$  ppt) at 100 m depth. At Station 14 (also obtained during late summer)  $S$  was slightly higher, the range of  $\theta$  was about  $19.5^\circ\text{C}$  to  $15^\circ\text{C}$ , and the AW layer was only 50 m thick. During winter, stations 17 and 63 showed only a small decrease in  $\theta$  with depth through their AW layers, although the thicknesses of the AW layers were similar to stations 10 and 14, respectively (Fig. 11).

Across the transition zone beneath the AW  $\theta$  decreased from  $15$ – $16^\circ\text{C}$  to about  $13^\circ\text{C}$ , and salinity increased from near 36.5 ppt to 38 ppt. Below the transition zone the changes in  $\theta$  and  $S$  were small, but these subtle differences are important because they delineated the Mediterranean water masses (see Fig. 12 inset). A  $\theta$  minimum ( $\sim 12.90^\circ\text{C}$ ) located near 200 m at stations 17 and 63 was similar to that found by Lanoix (1974) in 1962. As noted, this minimum has been either very small or entirely absent in recent years.

Between 200 m and 600 m depth the  $\theta$  and  $S$  maxima related to LIW were present and were diminished from their maximum values in the eastern Mediterranean. In Figure 12 the  $\theta$  maximum occurred about 100 m above the  $S$  maximum, and at station 14 several maxima occurred between 200 and 300 m depth. These multiple maxima were found in many continuous profile (CTD) stations made in the western Alboran in 1981 and 1982. These maxima would probably have been missed by earlier discrete bottle sampling, but they appear to be a common feature. The  $\theta$  maxima ranged from  $13.10^\circ$  to  $13.20^\circ\text{C}$  and the  $S$  maxima from 38.46 to 38.50 ppt. LIW at the Strait of Sicily may have values of  $14^\circ\text{C}$  and 38.7 ppt (Katz, 1972), so the LIW has mixed with its neighboring water masses significantly before arriving in the Alboran. Comparing different years and sources, the maxima seem to vary by no more than  $0.10^\circ\text{C}$  and 0.03 ppt. The potential density of the intermediate water occurs near  $\sigma = 29.08$   $\text{kg}/\text{m}^3$ . Below the LIW,  $\theta$  and  $S$  decrease slowly, reaching  $\theta = 12.74^\circ\text{C}$ ,  $S = 38.425$  ppt and  $\sigma = 29.11$   $\text{kg}/\text{m}^3$ ; from the LIW core at 350 m to the greatest depth in the western Alboran ( $\sim 1600$  m) the  $\theta$ - $S$  curve nearly parallels the  $\sigma_\theta = 29.10$  isopycnal.

The DW values have not varied much in recent years and seem to have been constant within the accuracy of instrumentation and the resolution of sampling. The AW and LIW, however, do show changes and these changes result from their values at formation, their rate of formation, and especially their modification subsequent to formation. These water masses may undergo significant modification and geographical variation while they are in the Alboran.

## C. Atlantic Water: the anticyclonic gyre and its variability

### 1. The geographic distribution of Atlantic Water.

Most of the Alboran Sea is covered by a shallow layer of AW, although its original characteristics are modified by heating, cooling, evaporation, and mixing with Mediterranean waters. North Atlantic Central Water (Sverdrup et al., 1942) and surface Atlantic water enter the Western Alboran Sea through the Strait of Gibraltar. These inflowing waters, which undergo some mixing while in the strait, are characterized by a vein of relatively low salinity and by a different temperature (relatively cooler in summer and warmer in winter). A series of eddies and meanders exist on both sides of the vein of AW. This vein moves swiftly northeastward after passing through the strait, more or less along the axis of the Strait. Between  $3^\circ$  and  $4^\circ\text{W}$  it turns southward, crosses the sea, and bifurcates. One branch returns westward describing an anticyclonic gyre; the other continues eastward, crosses the  $3^\circ\text{W}$  meridian, forms meanders,

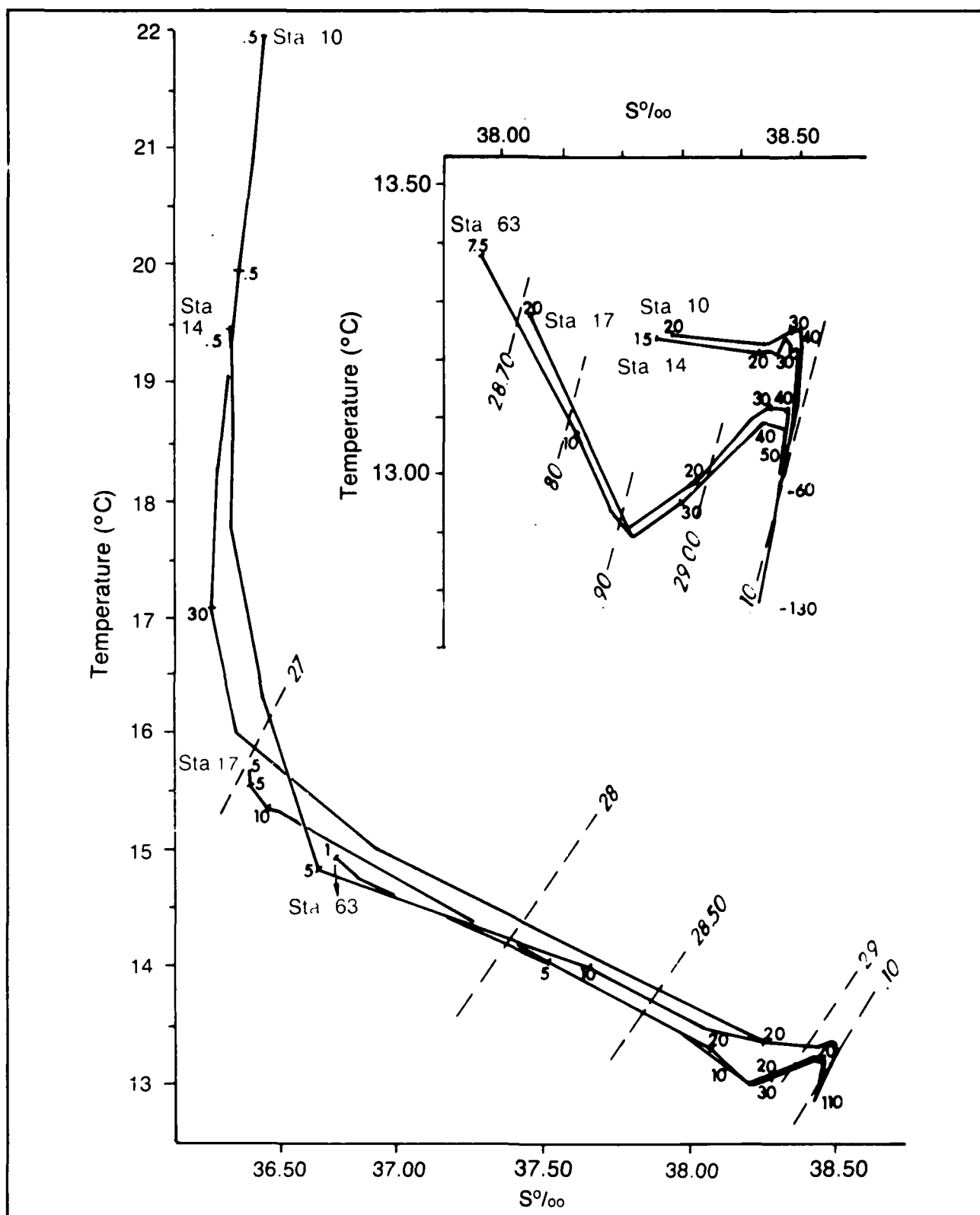


Figure 12. Temperature-salinity curves for the stations shown in Figure 1

and outlines a variable number of eddies. This branch hugs the Algerian Coast as it progresses eastward.

When the current vein enters the Alboran, it creates one of the most pronounced fronts in the Mediterranean on the northern edge of the gyre, dominating the Western Alboran Sea. This front is confined to the upper 200 m and has a width of about 30 km. Its horizontal gradients of surface temperature are stronger in summer and early autumn ( $0.1^{\circ}$  to  $1.0^{\circ}\text{C}/\text{km}$ ) than in the rest of the year ( $\sim 0.05^{\circ}\text{C}/\text{km}$ ). The salinity gradient is  $0.03$  ppt/km at 100 m and the seasonal variations are small (Cheney and Doblar, 1982). The total changes across the front are about  $4^{\circ}\text{C}$  near the surface in summer and about 1 ppt at 100 m throughout the year.

Figure 13 shows isotherms and isohalines at 30 and 100 m, and the depth of the 37.5-ppt surface in April 1980 (the 37.5-ppt isohaline is often arbitrarily chosen as the boundary between Atlantic and Mediterranean waters). The shallow vertical and horizontal temperature gradients were weak, both as a result of winter cooling and of strong winds. The picture at 30 m was complicated. South of  $36^{\circ}\text{N}$  and west of  $3^{\circ}\text{W}$  generally warmer and fresher water was in contact with a colder and saltier region to the north. Several isolated patches of water of different characteristics were embedded in both these regions.

At 100 m the picture was much clearer. The axis of the front ran along the  $36^{\circ}\text{N}$  parallel bordering the gyre, which was displaced to the south from Lanoix's (1974) classical description. Warm and fresh AW ( $15.35^{\circ}\text{C}$ , 36.40 ppt) existed at the core of the gyre. Farther east the front defined a meander that passed north of Alboran Island, enclosing an AW colder and saltier than that of the gyre. East of Alboran Island the isohalines turned southward and then continued eastward near Cabo Tres Forcas. Cheney and Doblar (1982) showed a similar 100-m salinity distribution for October 1977, but their gyre extended farther northward and the stronger salinity gradient was south instead of north of Alboran Island.

While the salinity distributions at 30- and 100-m depths suggested the same location for the gyre center, temperatures at 30 and 100 m did not. The 30-m thermal center was displaced eastward, and the 100-m thermal center was coincident with the salinity distributions. Inside the gyre and the meander the 37.5 ppt surface reached its greatest depths—more than 200 m and 120 m, respectively. The southern branch of the cooler, saltier side of the front, which might be expected to surround the warmer and fresher gyre core, was not present, although the cooler, saltier patch against the Moroccan coast southwest of the gyre may have been a trace of it.

In the Alboran literature considerable interest has been shown in the regions just northeast and just southeast of the strait. South of Punta Almina the

isolines and the depth of the 37.5 ppt surface seemed to imply that AW flowed southward along the African Coast before becoming trapped in the gyre (Fenner, 1979). Lanoix (1974) explained the existence in that zone of an anticyclonic eddy in the confluence of the inflowing AW and the westward current south of the gyre. Most hydrographic data, however, have not resolved the detailed structure of this small region, and some of the data have probably been aliased by tides.

Northeast of Gibraltar a cold region is often present along the Spanish Coast, which indicates possible upwelling (Lanoix, 1974; Cano, 1977; Copin-Montegut et al., 1981). This cold region also appears in nearly all summertime satellite infrared images. Some authors (e.g., Cano, 1978b) have written about the existence of a cyclonic eddy in that zone. Others (Stevenson, 1977; Gallagher et al., 1981) have discussed the possibility of water upwelled along the Cadiz Coast in the Atlantic being advected by the Atlantic inflow. The average wind stress along this coast is toward the east and creates conditions favorable for upwelling (Fig. 9). In cruises made during the last two years by the Instituto Español de Oceanografía (IEO) and the Naval Ocean Research and Development Activity (NORDA), there was some hydrographic evidence for a narrow surface divergence near  $5^{\circ}\text{W}$ . Evidence of cold temperatures and high salinities ( $> 37$  ppt at 10 m in June 1982) is adequate enough to know that subsurface waters routinely appear at the surface off the Spanish Coast (Fig. 14). It is not known how these waters arrive there, whether the upwelling process is local, or whether it occurs elsewhere.

Although most of the AW flows into the Eastern Alboran Sea Basin south of Alboran Island, a sporadic substantial flow is located north of the island (Lanoix, 1974). In June 1982 volume transports inferred from hydrographic sections showed that of  $1.3 \times 10^6$  m<sup>3</sup>/sec inflowing,  $0.9 \times 10^6$  m<sup>3</sup>/sec continued eastward north of the island.

Figure 15 shows a different season (October 1981) and also shows distributions in the eastern basin. We added the subsurface salinity minimum to the parameters used in Figure 13 so that the probable path of the AW could be visualized. The distance between stations was greater than in April 1980, but the main features were still found.

At 10 and 100 m the existence of the gyre was evident. In this case it was warmer and wider than in April, although the northern part was slightly colder and saltier. At 10 m there was a fresh tongue of AW in front of the strait and relatively fresh water close to the Spanish Coast, southwest of Malaga. The anticyclonic meander was found again, but this time farther east near  $1^{\circ}30'\text{W}$ ; dimensions and values were similar to the anticyclonic gyre in the west. Both hydrography (Lanoix, 1974; Cano 1977, 1978a) and satellite imagery (Phillippe, 1980) indicate that this



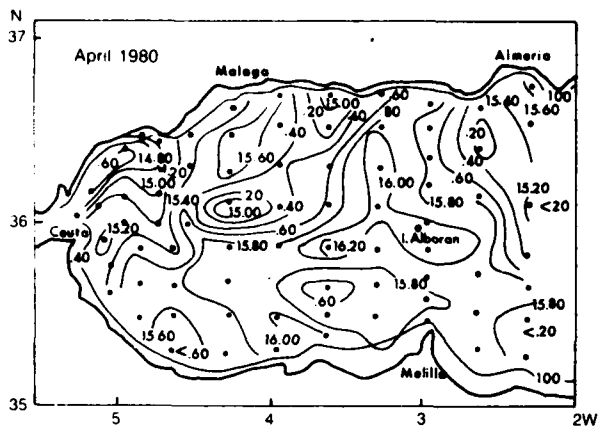


Figure 13(a). Temperature at 30 m depth during the Cornide de Saavedra cruise in April 1980.

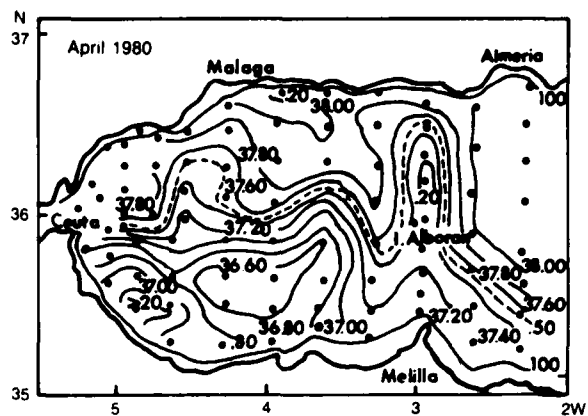


Figure 13(d). Salinity at 100 m depth during the Cornide de Saavedra cruise in April 1980.

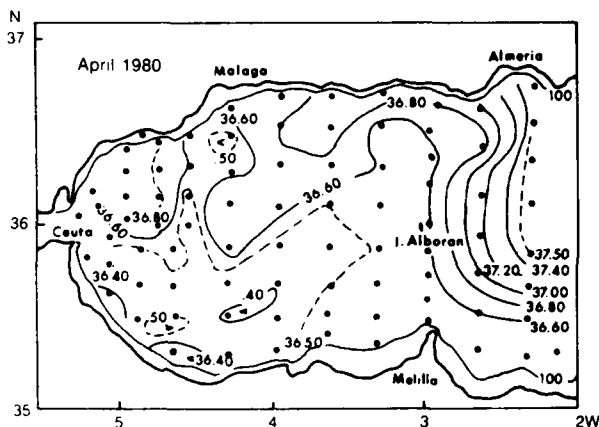


Figure 13(b). Salinity at 30 m depth during the Cornide de Saavedra cruise in April 1980.

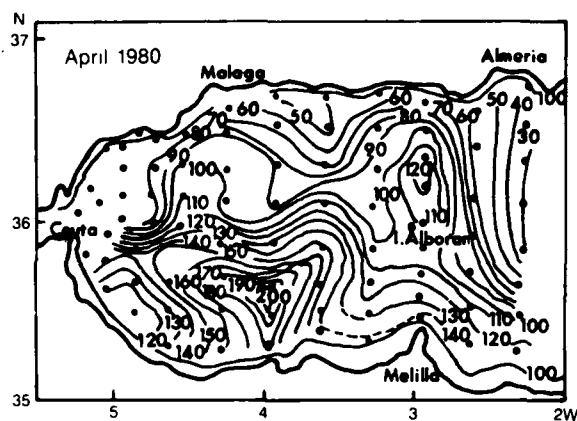


Figure 13(e). Depth of the 37.5 salinity surface during the Cornide de Saavedra cruise in April 1980.

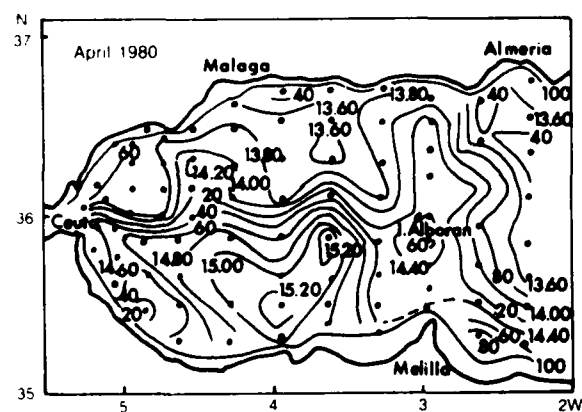


Figure 13(c). Temperature at 100 m depth during the Cornide de Saavedra cruise in April 1980.

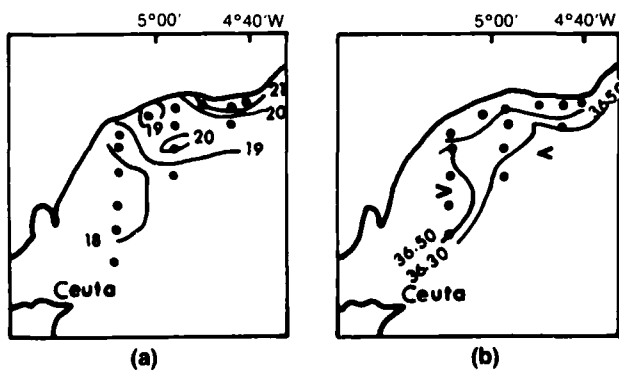


Figure 14. Temperature (a) and salinity (b) at 1 m depth during August 1982 (redrawn from J. Gil, Instituto Español de Oceanografía, Malaga).

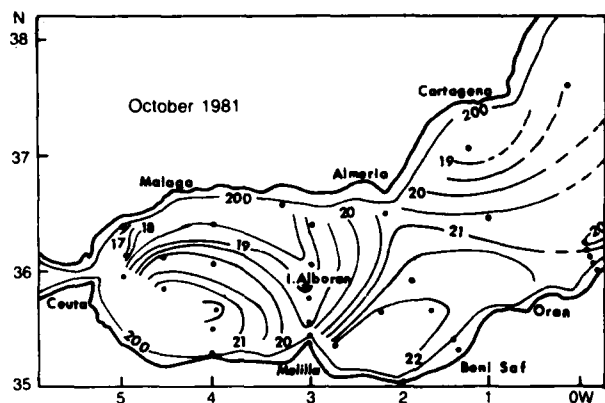


Figure 15(a). Temperature at 10 m depth during the Cornide de Saavedra cruise in October 1981.

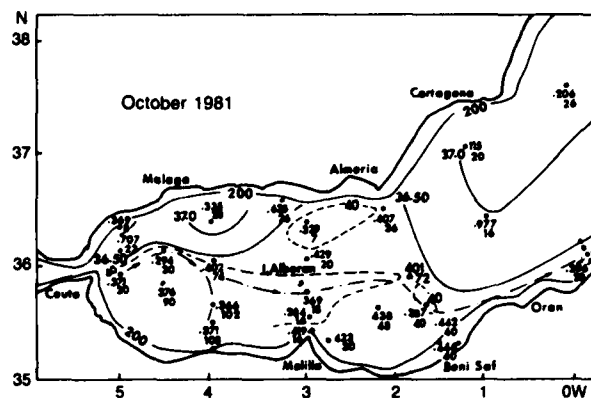


Figure 15(d). Salinity at 100 m depth during the Cornide de Saavedra cruise in October 1981.

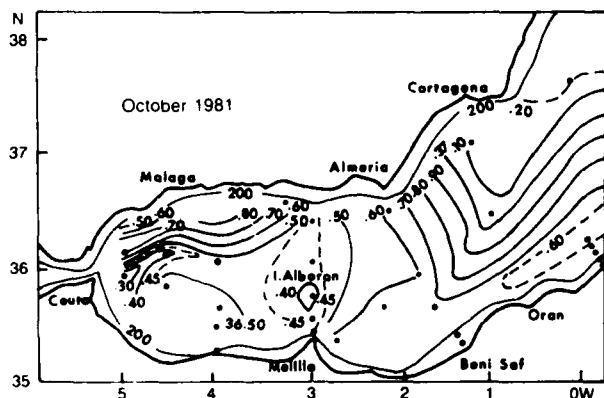


Figure 15(b). Salinity at 10 m depth during the Cornide de Saavedra cruise in October 1981.

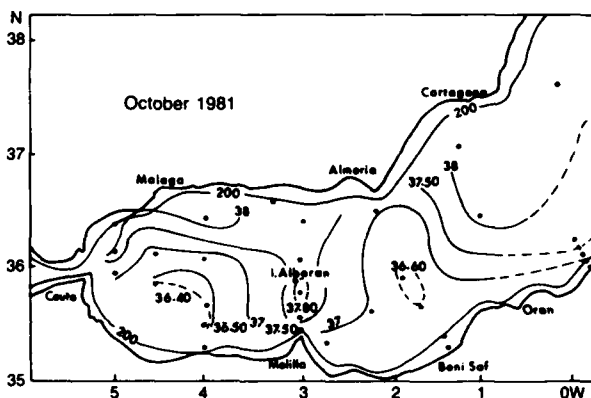


Figure 15(e). Depth of the 36 salinity surface during the Cornide de Saavedra cruise in October 1981.

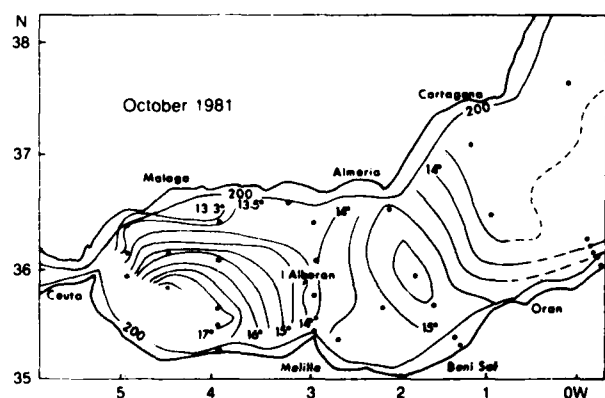


Figure 15(c). Temperature at 100 m depth during the Cornide de Saavedra cruise in October 1981.

meander is an intermittent feature that can be found in different locations and can sometimes disappear. From the point where the eastern side of the meander reaches the African Coast, the Atlantic Current

continued eastward and stayed close to the coast. At the location of the anticyclonic meander in April 1980, there was a cyclonic feature with high salinity and low temperature in its core. This distribution appeared similar to the 1962 distributions (Lanoix, 1974).

In the salinity minimum distribution we have drawn an axis that follows the lowest values. The lowest salinity (36.29 ppt) was found on the southern border of the front at 30 m (around 4°30' W). Near 4°15' W an axis that circled the gyre increased its depth (reaching values greater than 100 m) and eventually spiraled into it. The other axis continued eastward south of the island; the salinity increased slowly and steadily, and its depth decreased to less than 20 m except in the meander; here, it increased to 40 m and maintained that depth as it hugged the Algerian Coast.

North of the island there was a wide zone where the minimum was nearly the same as near Gibraltar and the gyre, but shallower. Lanoix (1974) described a similar picture and drew a third axis north of the island that joined the eastward axis. Our pattern may be the same, but we do not have the data to confirm it.

Before ending this section we would like to present a picture (redrawn from Cano, 1978b) where the AW distributions for different years during the same season are shown (Fig. 16). He classified the  $\theta$ -S curves by the influence of AW (Fig. 16a), labeling them from *a* to *e*, where *a* is the most AW-influenced and *e* the least. It can be seen that while some general features can be found in all years—e.g., more Atlantic-influenced water to the west and south of the Alboran Sea—no general seasonal pattern emerges.

**2. The anticyclonic gyre and its variability.** Field data gathered in the last 20 years from ships, historical files, and satellite imagery establish the anticyclonic gyre as a permanent feature with great variability (Wannamaker, 1979). In general the gyre has a nearly circular shape, but there is a meridional asymmetry: the zonal axis is south of the 36°N parallel, and the strongest gradients and flows are found in the north. In a vertical profile the isolines form a bowl whose diameter diminishes with depth (Fig. 17). The horizontal scale is 100 km and the vertical scale is 200 m. Data show that the gyre can shift position as much as 50 km and its area can vary by a factor of two (Cheney and Doblar, 1982). The vertical scale does not seem to suffer such dramatic changes. The inner part of the gyre is occupied by low-salinity AW with an almost isohaline layer (36.4–36.5 ppt) reaching more than 100 m and where the depth of the salinity minimum is greater than in the rest of the sea. This water is warmer than its surroundings, although surface temperature contrasts with the AW inflow are small in winter (e.g., Philippe and Harang, 1982, Fig. 22). The slopes of the isolines in the northern part are about 2.2 m/km for the 15°C isotherm and 2.6 m/km for the 37 ppt isohaline (Parrilla and Salat, 1982).

Several theories have been given to explain the presence of the gyre (Lanoix, 1974; Ovchinnikov et al., 1976; Nof, 1978; Whitehead and Miller, 1979; Preller and Hurlburt, 1982; Bryden and Stommel, 1982). Lanoix (1974), using the theoretical studies of Saint-Guilley (1957) and employing very simple conditions, explained the meandering of the Atlantic vein and gave a qualitative indication of the sinuosity of the trajectory and probable formation of gyres. Ovchinnikov et al. (1976) suggested that the gyre is produced by a particular wind field, but this is not a tenable solution now that the permanence of the gyre is known (Whitehead and Miller, 1979).

Nof (1978) used an analytical model and laboratory experiments to investigate the behavior of flows exiting from straits. With uniform horizontal velocity profiles in the current leaving the strait, he found that the currents tended to turn to the right in the Northern Hemisphere, in agreement with intuition. For the case where large negative relative vorticity was imposed, however, the flow turned to the left. He suggested that the Atlantic water entering the Alboran Sea might be an application for this solution.

Whitehead and Miller (1979) reproduced the gyre in a transient laboratory experiment consisting of two basins, which were connected by a channel, on a rotating turntable. After the flow was initiated between the two basins, a jet formed that separated from the curved wall. An anticyclonic gyre was observed between the jet and the wall. The jet and the gyre initially were both a Rossby radius in size, but gradually the gyre grew larger, apparently from an accumulation of fluid from the jet as it returned to the wall. This growth appeared to be linked with a filling process related to the dynamics of the stagnation point of the jet as it impinged on the modeled coast of Africa. In one of the steps of this experiment realistic coastline features were simulated and a similar result was found.

Preller and Hurlburt (1982) used a reduced gravity model (active upper layer, quiescent lower layer) for the Alboran basin. The Strait of Gibraltar was simulated by a port in the western boundary, and the eastern boundary was entirely open. The formulation did not include bottom topography, coastline features, or winds. The model was forced by the Gibraltar inflow, and the solution evolved to a steady state that exhibited a meandering eastward current. The first meander of this current formed the northern boundary of a strong anticyclonic gyre in the western part. An initial investigation using this model indicated the importance of the inflow angle, inflow vorticity, inflow speed, and the location of the strait. The meandering current observed in the model solutions might be considered a standing Rossby wave with a highly distorted conservation of absolute vorticity trajectory.

Bryden and Stommel (1982) noted that to maintain the anticyclonic gyre in the presence of friction, a source of anticyclonic vorticity is required. This source could be provided by a flow of western Mediterranean deep water upward and toward the strait. The possibility of such a flow was pointed out by Stommel et al. (1973), who used a Bernoulli argument to show how high velocities in the strait could raise water from great depth in the Mediterranean up and over the sill. This upward flow of DW and concurrent vortex shrinking provides the necessary source of anticyclonic vorticity to maintain the gyre which, in turn, provides the necessary energy for raising the deep water in the Alboran Sea.

It is interesting that the ideas about the gyre are so diverse, at least in some of their details. For instance, a steady-state, angled (north of east) inflow, rectangular wall experiment (Preller and Hurlburt, 1982) showed similar results to a transient straight inflow experiment (Whitehead and Miller, 1979) in which the interaction of the boundary and the jet appeared to be critical. The vorticity mechanism proposed by Bryden and Stommel (1982) cannot be simulated in the Preller and Hurlburt model. Nevertheless, future modeling, which will include a planned expansion of

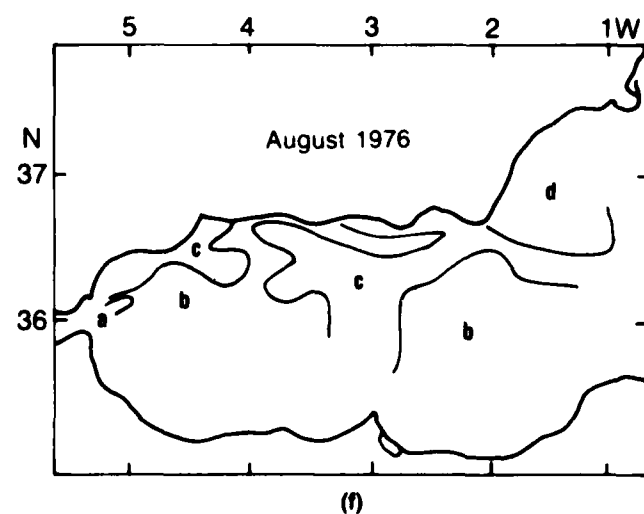
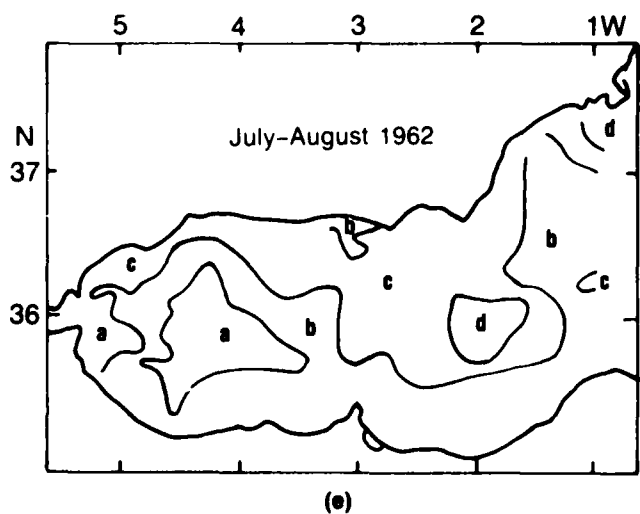
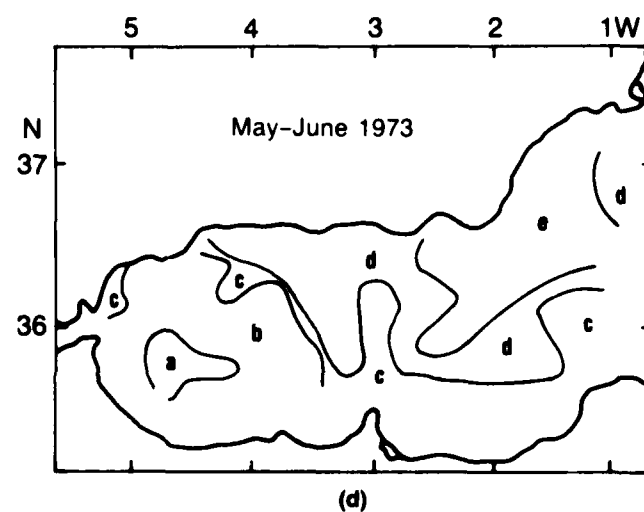
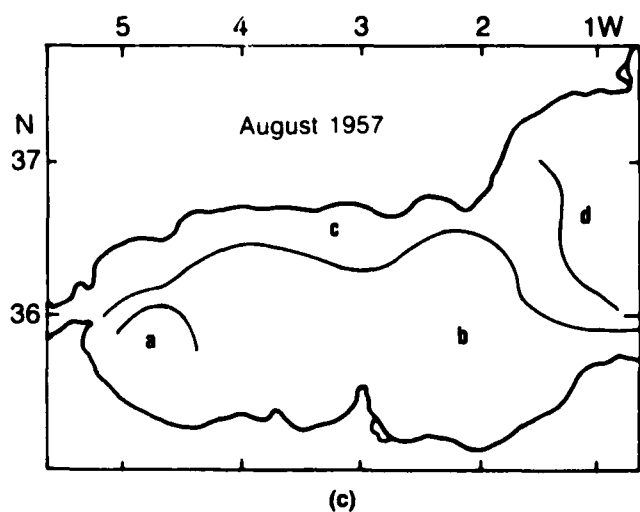
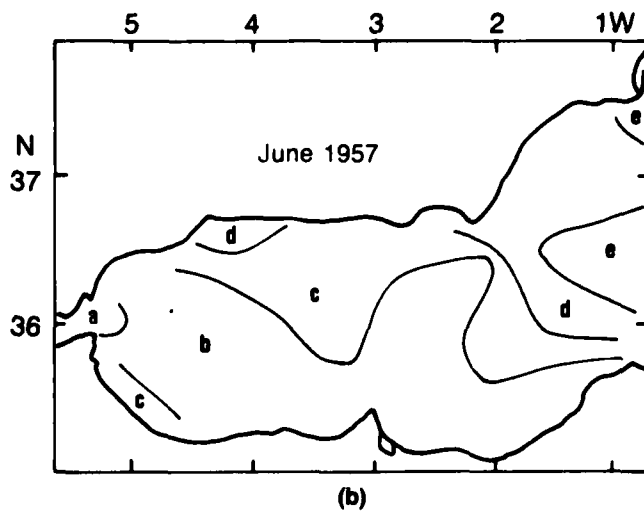
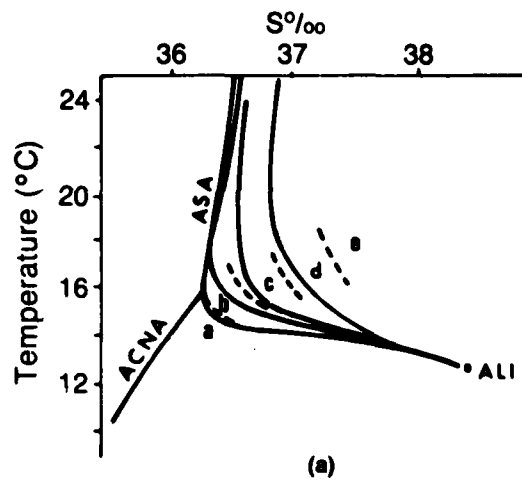


Figure 16(a). Classification scheme for the Atlantic Water devised by Cano (1978b). (b-f). Geographic distribution of the Atlantic Water during various cruises according to Cano.

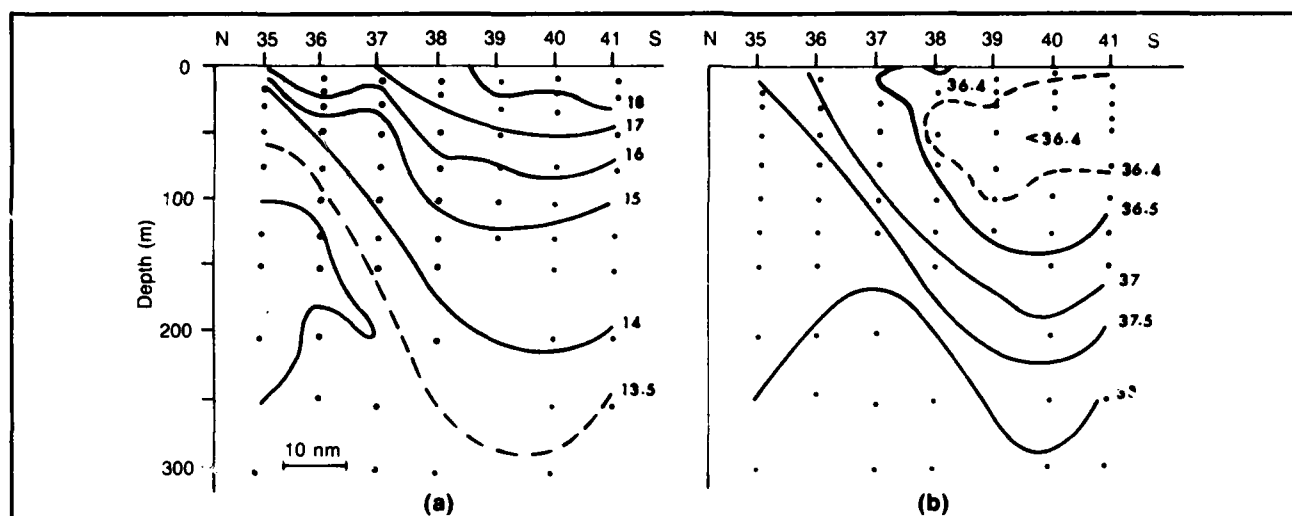


Figure 17. (a) Temperature and (b) salinity section along 4°W during May-June 1973 (Cano, 1977, section VI).

the Preller and Hurlburt model (personal communication), should result in a better understanding of the dynamics of the gyre.

The gyre has displayed strong variability. Cheney and Doblar (1982) reported a 50-km translation of the gyre and sensible variations of its area within 10 days. Gallagher et al. (1981) mentioned significant changes of 2°C at fixed locations in 1 or 2 hours at depths as great as 200 m, and isotherm excursions at depths from 20 to 50 m. They also reported 2°C changes over horizontal distances of 5.5 to 9 km in less than one day, and lateral shifts of water mass boundaries from 3.5 to 7 km in a few hours. They presented a satellite image series for several days where progressive and regressive excursions of the AW tongue are shown. No recognizable surface expression of the gyre was present on one day. They also noted that changes in the position of the tongue and the interior of the gyre did not necessarily occur in unison.

La Violette (1983) used a series of twice-daily satellite infrared images from 5 to 20 October 1982 to track cold-water features around the gyre. The features apparently began as a 10-km southward bulge of colder surface water near the strait, which were then advected around the gyre at a mean speed of 0.4 m/sec. These features, which also measure about 10 km in the downstream direction, appear in satellite imagery from other periods and had a significant subsurface extent during October 1982. Their importance to the gyre dynamics is not known, but they probably make a significant contribution to the temporal and spatial variability, and to aliasing of conventionally gathered data.

Fluctuations in the gyre may be strongly linked to fluctuations of the inflow of AW, as some of the models suggest. Long-term (i.e., seasonal and inter-annual) fluctuations are caused by variations in the density and sea level differences between the North

Atlantic and the Mediterranean (e.g., evaporation rate). Shorter term fluctuations are probably caused by tides, wind stress, atmospheric pressure and, perhaps, internal waves. It is believed that the maximum inflow is in summer (Carter, 1956; Cano and Fernandez, 1968; Ovchinnikov, 1974), although the higher evaporation is in winter (Lacombe and Tchernia, 1972; Bunker, 1972). In summer the prevailing wind field is variable in direction and easterly winds are frequent, but in other seasons it is westerly (See Section III). There is some evidence that both strong inflow and easterly winds will favor a larger gyre, but evidence is not sufficient enough to confirm this.

#### D. The temperature minimum layer

Above the LIW near 200 m depth lies a temperature minimum layer. Lanoix (1974) attributed this layer to water formed in the northern Algero-Provençal basin in winter. This cold, moderately saline water reaches its equilibrium density above the more haline LIW. This water may be linked to *eau d'hiver superficielle de la Riviera* because of its temperature and salinity of 12.35°C and 38.3 ppt (Lacombe and Tchernia, 1960). Katz (1972) mentioned the existence of a similar water mass (12.65°C, 38.15 ppt) south of the Balearic Channel (near 37°10' N) between 160 and 325 m depth during July 1970. This water apparently contributed to the dilution of the westward-flowing LIW. Lanoix (1974) showed values as low as 12.72°C (38.15 ppt), and Bryden et al. (1978; see our Fig. 13) measured potential temperatures between 12.9° and 13.0°C (38.21–38.30 ppt).

In the cruises made by the Instituto Español de Oceanografía during the late 1970s and early 1980s, this layer was also detected, but with some changes. Three pictures of the horizontal distribution of this minimum for different seasons and years are presented in Figure 18. The distribution of this water has some

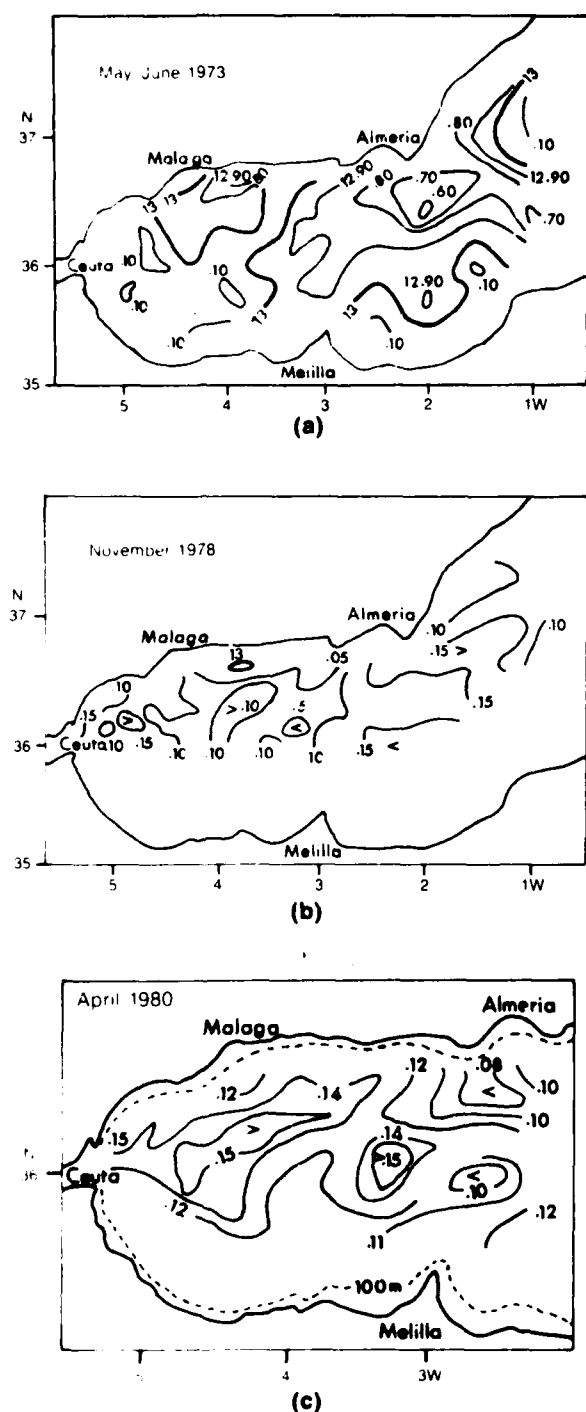


Figure 18. Temperature at the minimum during (a) May-June 1973, (b) November 1978, and (c) April 1980. The temperatures in (b) and (c) are greater than  $13^{\circ}\text{C}$ . Data in (a) and (b) are from Cano and Gil (1982).

similarities to that of the LIW. It apparently flows westward, mainly in the northern half of the basin, and its distribution is cell-like. Temperature increases to the west and to the south. The 1973 picture shows values similar to those that Bryden et al. (1978) found

in 1975. In 1978 and 1980, however, there was a general warming and an increase of the salt content. The 1978 potential temperatures varied between  $13.00^{\circ}\text{C}$  and  $13.10^{\circ}\text{C}$ , with some spots reaching  $13.15^{\circ}\text{C}$ . In 1980 the lowest minimum, northeast of Alboran Island, was  $13.07^{\circ}\text{C}$ , and although temperatures did not reach values much higher than  $13.15^{\circ}\text{C}$ , they were generally higher than in 1978. The salinities were around 38.25 ppt. In a cruise made in October 1981 by the *Cornide de Saavedra*, the lowest potential temperature in the eastern limit of the Alboran Sea (Station 26, Fig. 12) was  $13.10^{\circ}\text{C}$  and the salinity was 38.33 ppt. During the Donde Va experiment in June 1982 (Kinder et al., 1983), the potential temperature minimum was only hundredths lower than the LIW maximum and the salinity was over 38.40 ppt.

Apparently the temperature and salinity of this layer has varied importantly over the last two decades. Part of the importance of this layer is its influence on the underlying LIW, which we discuss in the next section.

### E. The Levantine Intermediate Water

Nielsen (1912), Wust (1960, 1961), and others established the existence of an intermediate layer of high salinity and temperature in the Mediterranean Sea. Its origin is in the Rhodes-Cyprus area, where a 150-m-thick homogeneous layer, characterized by elevated salinity and temperature (39.1 ppt,  $15^{\circ}\text{C}$ ; Morcos, 1972) is formed during winter. It subsequently spreads throughout the Mediterranean, and its properties deteriorate during its westward movement. After crossing the Strait of Sicily (at 38.74 ppt and  $<14.35^{\circ}\text{C}$  in the bottom of the strait during winter) the Levantine Intermediate Water (LIW) follows three main courses in the western Mediterranean (Katz, 1972; Garzoli and Millard, 1979). After completing these three circuitous courses it enters the Alboran Sea and finally contributes to outflow through the Strait of Gibraltar.

When it reaches the Alboran Basin its signature has weakened, and it diminishes more on its way to Gibraltar within the basin; but it is still possible to detect the maxima that have distinguished the LIW in its spreading throughout the Mediterranean Sea. In contrast with the findings of other authors (Lacombe and Tchernia, 1960; Lanoix, 1974), we found that the properties of the LIW were quite recognizable in most of the Alboran Sea during our recent cruises, except in the southernmost part near the Moroccan and Algerian coasts. One reason for a better perception of LIW in a broader area than in past years is the refinement in the measuring techniques employed. Until recently the sampling methods used in the Alboran Sea consisted mainly of lowering Nansen bottles or other devices for spot sampling at selected depths. The working difficulties presented by the strong currents in the region and the quasi-homogeneity of the water column from some 300 m to the bottom, together with the spot

sampling, inhibited the recognition and identification of the LIW layer. With present methods, which are capable of a higher resolution, a better knowledge of the water column is assured. Furthermore, the values of the maxima in the last four years apparently are higher than those of the 1960s and early 1970s, which also helps their identification.

The LIW layer is normally found between depths of 200 m and 600 m. Occasionally more than one distinct layer has been observed, mainly in the western part. Where there are several layers, one dominates over the others. As mentioned, the salinity maximum is about 100 m below the temperature maximum. This displacement is a natural consequence of diffusion and of the condition of the equation of state on the TS plane, but it also appears to imply an unequal rate of mixing, which suggests that layers at different levels may be more affected over than others. The vertical gradients of potential temperature between the LIW and the overlying water masses are weaker than temperature gradients below, but the opposite condition holds for the gradients of salinity.

In its westward movement the S and  $\theta$  maxima decrease in a parallel evolution. The changes in the properties are not strong enough to mask the LIW, even in the strait. This suggests that mixing with the other water masses is not very active (Katz, 1972; Bryden and Stommel, 1982), at least not everywhere. In Figure 19 several  $\theta$ -S curves are given, which show the evolution of the maxima in October 1981 between the parallels  $1^{\circ}47'W$  and  $5^{\circ}W$ , more or less along the  $36^{\circ}N$  meridian.

The LIW entered the Alboran Sea concentrated in the northern part (Fig. 20). Its path in the eastern basin did not cross south of  $35^{\circ}30'N$ . In the region between Cabo Tres Forcas and Cabo Figalo, where there is a relatively broad shelf, no traces of the maxima have been found (Figs. 20 and 21; Lanoix, 1974, Fig. 16). Upon crossing the  $31^{\circ}W$  meridian near Alboran Island, it passed on both sides of the island. The bulk passed to the north, where the higher maxima and thicknesses were found. Between this meridian and the strait the LIW signature was stronger in the northern half of the basin. The LIW moves near the Spanish coast on its way toward the strait, where the horizontal gradients of its properties increase noticeably due to encountering the inflowing Atlantic water. Near the strait it is difficult to estimate the proportionate contributions of the different water masses because of the strong tidal fluctuations. It seems that in the African corner between Ceuta and  $4^{\circ}W$ , the LIW has no influence, although its signature may be obscured by the DW, which has a strong presence in that zone (Bryden and Stommel, 1982; see our Fig. 22). In the zone of the gyre the shape of the isolines of the LIW suggests a cyclonic movement, which will be discussed in section V.

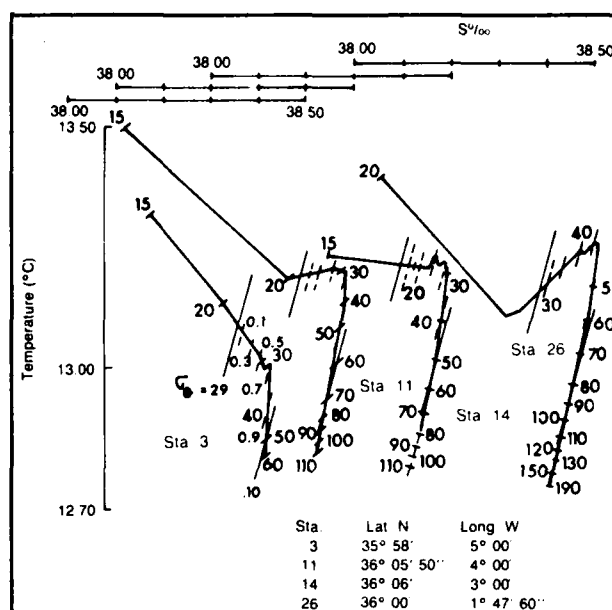


Figure 19. Temperature-salinity curves showing the variation of the salinity maximum during the Corvide de Saavedra cruise in October 1981. Depths in decameters.

During recent years a warmer and saltier LIW has been observed (Miller, 1982). We have found values of salinity near or equal to 38.50 ppt ( $\pm 0.005$ ) and potential temperature of about  $13.24^{\circ}C$  in the western Alboran, while the data from Projet Alboran I (Peluchon, 1965) during the summer of 1962 (used by Lanoix, 1974) fluctuated about 38.47 ppt and  $13.15^{\circ}C$  (in situ). Bryden et al. (1978) observed values of 38.47 ppt and  $13.10^{\circ}C$  (potential) for the winter in 1975. The augmentation of salinity is small, but the increase in the temperature is appreciable. Assuming that a climatological condition affects the formation of warmer and saltier LIW, it seems that the existence of the overlying "winter" water can strongly influence the LIW, especially the temperature values. Projet Alboran I and Bryden's cruise located a well-developed temperature minimum layer that was different from the situation found during our late 1970s and early 1980s cruises (see Section IV.4).

Furthermore, Wust (1961) established that the properties of the LIW had higher values in winter, a season close to our April (1980) cruise, but we found values very similar to those in April during our in October 1981 cruise (late summer situation). The Lanoix and Bryden data collected in summer (July 1962) and winter (February 1975) are more alike each other than to data from the more recent cruises. Perhaps the variation of these water masses are more strongly related to climatological fluctuations in their source regions than to the seasonal and yearly variability that we expected to find.

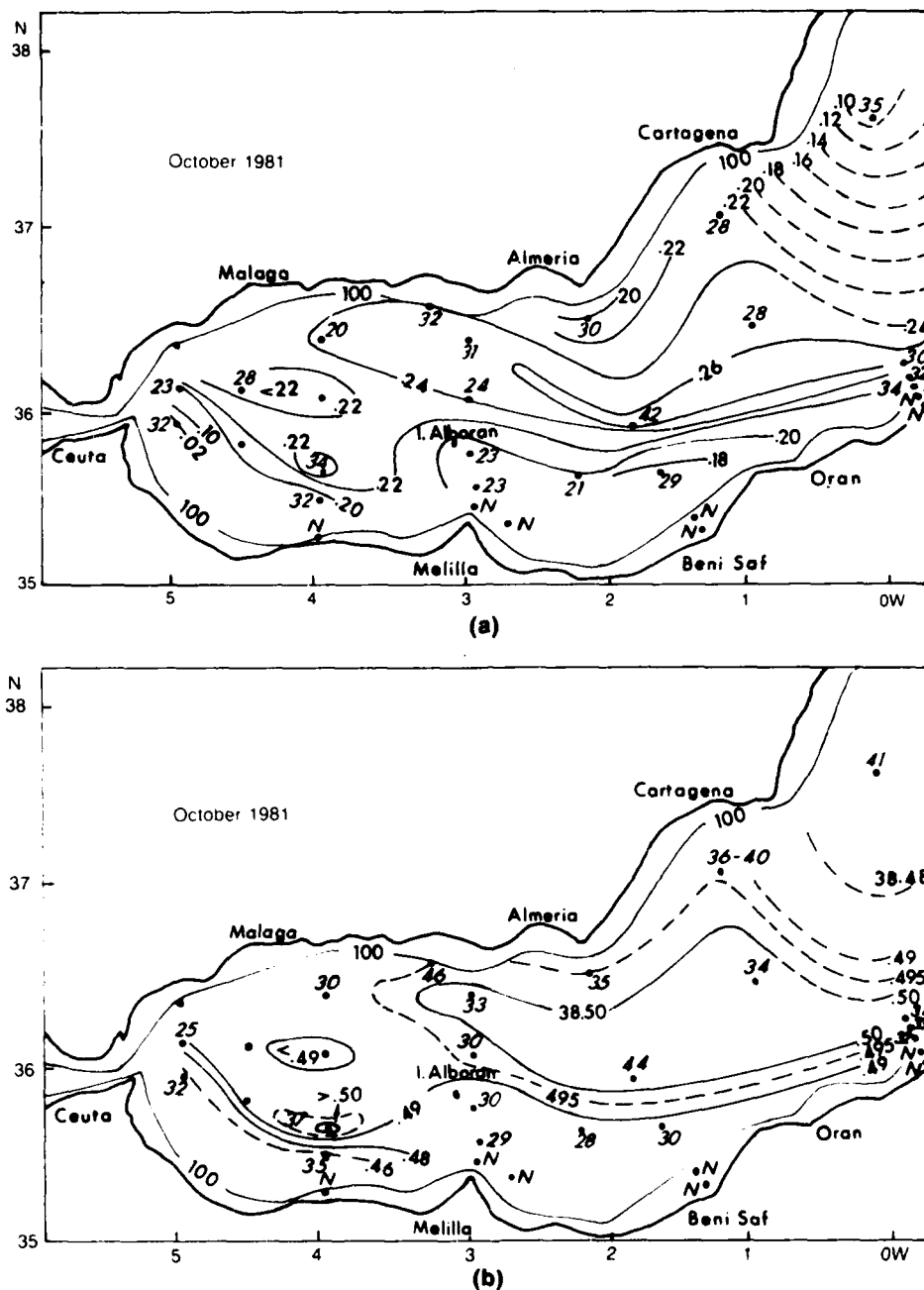


Figure 20(a). Temperature at the maximum showing Levantine Intermediate Water during the Cornide de Saavedra cruise in October 1981. Temperatures have  $13^{\circ}\text{C}$  subtracted from them (i.e.  $0.20 = 13.20$ ) and script numbers are depths in decameters. The letter "N" signifies no maximum. (b) Salinity at the maximum.

During June and October 1982, however, we found that the S maximum was about  $38.47\text{--}38.49$  ppt and the maximum was  $13.1^{\circ}\text{--}13.2^{\circ}\text{C}$ —intermediate between earlier lower values and the higher values in 1980–1981 data. There was no concomitant strengthening of the temperature minimum in 1982. It is likely that the strength of the temperature minimum layer is only one factor that influences the strength of the LIW in the western Alboran.

## F. The Deep Water

In the northwestern Mediterranean off the French Coast during winter, the climatological and oceanographic conditions favor processes of deep-water formation (Tchernia, 1960; Anati and Stommel, 1970; Sankey, 1973; Lacombe, 1974). After it is formed this water sinks and spreads southward, and fills the bottom layers of the Balearic, Alboran, and Tyrrhenian Seas (Wust, 1961; Ovchinnikov and Plakhin, 1965);



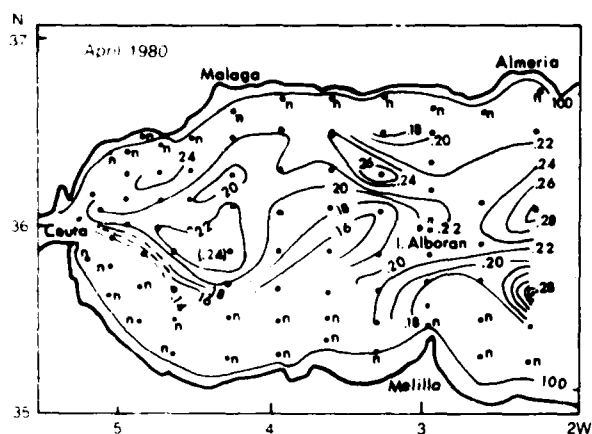


Figure 21. Temperature at the maximum showing the distribution of the Levantine Intermediate Water. The letter "n" signifies no maximum.

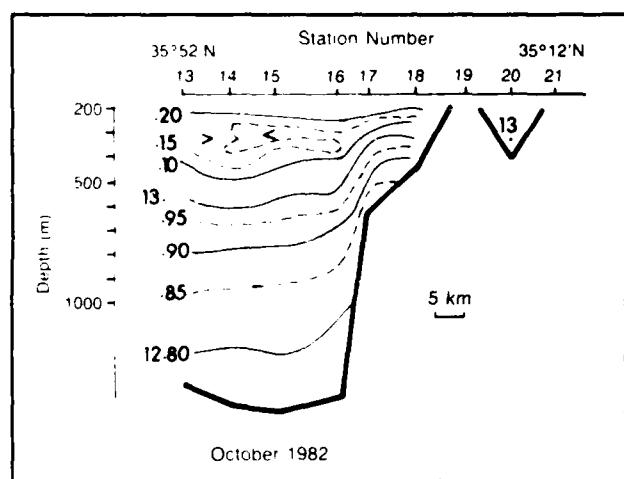


Figure 22. Potential temperature along 4°16'W during the Cornide de Saavedra cruise in October 1982.

eventually, part of it flows out directly through the strait (Stommel et al., 1973; Bryden and Stommel, 1982).

From the earliest measurements of the Deep Water (DW) (Nielsen, 1912) its properties have undergone little change. They oscillate around  $\theta = 12.70^\circ\text{C}$ ,  $S = 38.40\text{--}41$  ppt and  $\sigma_\theta = 29.105 \text{ kg m}^{-3}$ , but it appears that these values pertain to a DW that formed in previous processes and occupies the deep and bottom layers when new ones are forming; that is the reason some authors call it "old" DW. Obviously the old DW must have formed at the surface also, but intensive measurements in the MEDOC region thus far have always shown a "new" DW forming at a higher temperature than an old DW. Lacombe et al. (1981) gave the interannual variations for DW; it varies between  $12.91^\circ\text{C}$  and  $12.80^\circ\text{C}$  and between 38.415 ppt and 38.460 ppt, with higher values corresponding to milder winters. They also mention the existence of a

continuous mixing process of the newly formed DW with the old one, which results in a decrease in  $\theta$  and  $S$  of the newer. The volume of newly formed DW contributes less than one-fourth to the Gibraltar outflow (Lacombe, 1974), although in exceptional cases, e.g., during very cold winters, the formation rate is able to maintain the outflow for three years (Sankey, 1973).

For DW identification in the Alboran Sea we consider the water with a  $\theta$  less than  $12.90^\circ\text{C}$  and a  $\sigma_\theta$  of  $29.10 \text{ kg m}^{-3}$  or greater (Bryden and Stommel, 1982). In general (Fig. 23) the DW rises from east to west and from north to south. The east-west elevation is smooth (from 1200 m at  $2^\circ\text{W}$  to 800 m at  $4^\circ30'\text{W}$ ) until it arrives near the strait, where water with  $\theta$  identical to that of the DW south of the French Coast is about 100 m below the Gibraltar Sill (Bryden and Stommel, 1982). The depth changes from north to south are sharper, with differences of 400 m across the Alboran Sea. The DW isolines bank against the African Coast from as far east as  $0^\circ$  longitude, although the shallowest depths are found along the Moroccan slope near Gibraltar.

The shoaling of the DW ( $12.81^\circ\text{C}$ , 38.435 ppt, and  $29.11 \text{ kg m}^{-3}$ ) during October 1981 and during February 1975 is shown in Figure 24. In combining the 1981 cruise with Bryden's 1975 cruise, some reservations

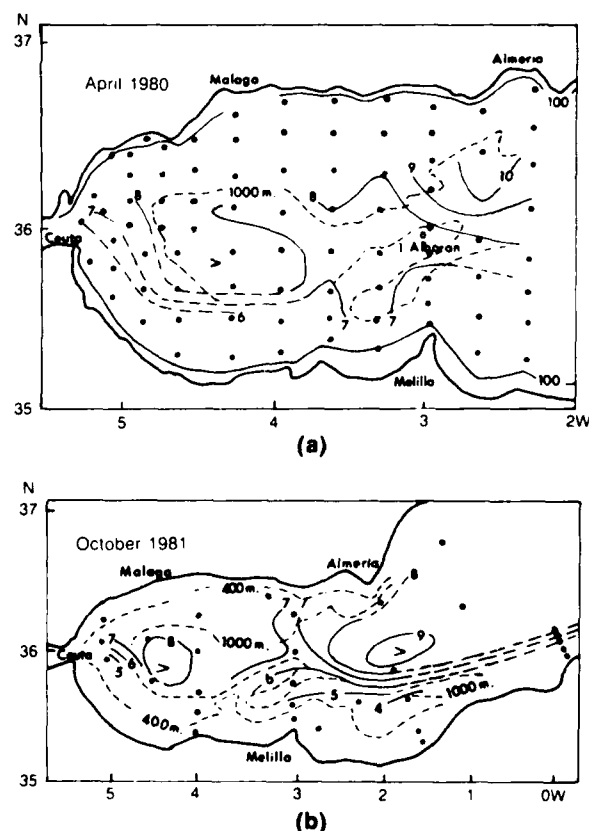


Figure 23. Depths of the  $12.90^\circ\text{C}$  potential temperature surface (hm) in (a) April 1980 and (b) October 1981.

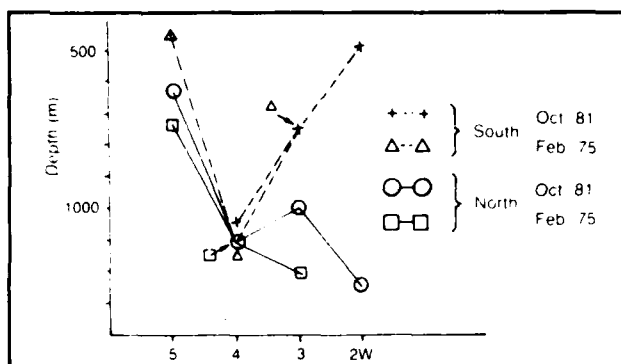


Figure 24. Depth of the potential isotherm  $12.81^{\circ}\text{C}$  versus longitude for the northern and southern half of the Alboran during Cornide de Saavedra cruises in February 1975 and October 1981.

should be noted. First, it was impossible to find stations at the same location for both cruises. Second, the distinction between southern and northern basins is arbitrary; it is actually a distinction between shallower and deeper DW depths.

Around  $4^{\circ}\text{W}$  the "northern" DW stays more or less at the same depth or it deepens slightly with respect to eastern water, but the "southern" DW sinks dramatically. We should be careful interpreting this. The cross-sectional area occupied by the DW that crosses north of Alboran Island increases, so that for the DW flow to be maintained, the depth (or speed) does not have to undergo big changes until it arrives at the strait. At the same time the anticyclonic gyre may have some influence. Unfortunately, we were not able to gather data nearer the Moroccan Coast, which should have shown DW at shallower depths, similar to those at  $3^{\circ}$  and  $5^{\circ}\text{W}$ . We also think that the particular bottom relief between Cabo Tres Forcas and Cabo Figalo, and the steep east-west slope of the passage south of Alboran Island (See Fig. 1) may enhance the rising of the DW near the African Coast.

## V. General circulation

### A. Atlantic Water circulation

A general idea of the circulation in the Alboran Sea can be deduced from the preceding section on the water mass distributions. The surface waters (AW) are animated by a net eastward movement, and the deeper waters (LIW and DW) by a net westward movement. Some of the deeper waters flows out over the Strait of Gibraltar sill. These motions can be inferred from the spatial evolution of the oceanographic characteristics and the horizontal pressure gradient which is generated by the decreasing of the mean sea level from the ocean to the Mediterranean by 10 to 15 cm between the two sides of the Strait.

According to Ovchinnikov (1966), the geostrophic circulation is fairly stable and "the surface circulation

and transport is wind-generated and make the most important contribution to the geostrophical transport. Currents at intermediate and deep layers are generated by thermohaline factors as well as by the wind." Burkov et al. (1979) gave some vertical profiles of the mean currents, which are characterized by a sharp decrease of the flow in the pycnocline (0–250 m). In the surface the velocity is higher than 50 cm/sec, decreasing to 1 cm/sec in the intermediate layer. They also found a slight maximum between LIW and DW, and finally a slight decrease to the bottom. According to both Wust (1961) and Ovchinnikov (1966) the rate of circulation in the surface and intermediate waters is lower in summer by a factor of about one-half. In the Alboran, this notion would appear to conflict with claims that the Atlantic inflow is strongest in summer (Carter, 1956; Cano and Fernandez, 1968; Ovchinnikov, 1974).

The distribution of stream lines in the surface layer (0–200 m) shows a pattern similar to that of the  $\theta$  and  $S$  isolines. Most of the direct and indirect current measurements made in this layer (Seco, 1959; Grousson and Faroux, 1963; Capart and Steyaert, 1963; Ovchinnikov, 1966; Lanoix, 1974; Parrilla, 1981; Gallagher et al., 1981) reveal a similar picture. Lanoix (1974) gave a very complete description of the surface circulation. Succinctly, the swift vein of incoming AW enters the Mediterranean following an east-northeast course, it turns south at around  $3^{\circ}3'0\text{W}$  and bifurcates south of  $36^{\circ}\text{N}$ . One branch circles the anticyclonic gyre, whose center is 20 or 30 dyn cm higher than the sea surface outside the gyre (Figs. 25 and 26). The other branch, which is the main part of the Atlantic current, usually passes south of Alboran Island in the eastern Alboran basin. In this basin the vein meanders, so on some occasions we found a great anticyclonic eddy (Fig. 26) near  $2^{\circ}\text{W}$  that separates the Atlantic flow from the African coast. Lanoix found that the flow can be pushed nearer this coast by a cyclonic eddy south of the Spanish coast (Fig. 25). In this case it seems that the size of the anticyclonic eddy has been reduced so that it occupies a very small area in a bight between  $1^{\circ}$  and  $3^{\circ}\text{W}$  (Cano, 1977). Lanoix has discussed the existence and causes of countercurrents (westward) near the coast in the same region. After this meandering the current hugs the Algerian coast and continues east.

As it flows into the Mediterranean, the Atlantic current widens and its velocity decreases. The higher speeds are found north of the western anticyclonic gyre, which is higher than 100 cm/sec in its periphery. In the western and southern branches of the gyre velocities appear to be about half those in the north. On both sides of the main current several eddies are formed, cyclonic to the left and anticyclonic to the right.

In addition to the large anticyclonic gyre that dominates the western Alboran, other eddies exist, such as the small one that apparently is often present south of Ceuta. This eddy is similar to the initial small gyre

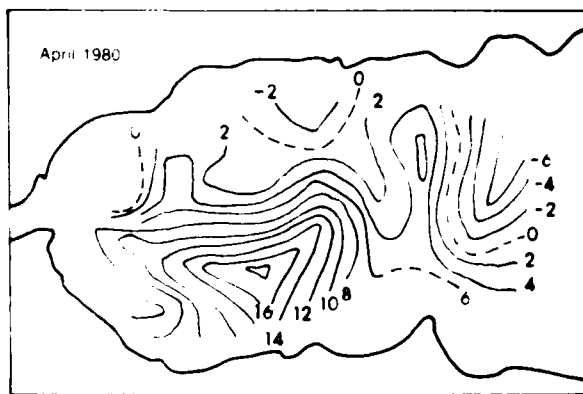


Figure 25. Dynamic topography of the surface relative to 200 dbar during Cornide de Saavedra cruise in April 1980 (dynamic cm).



Figure 26. Dynamic topography of the surface relative to 200 dbar during Cornide de Saavedra cruise in October 1981 (dynamic cm).

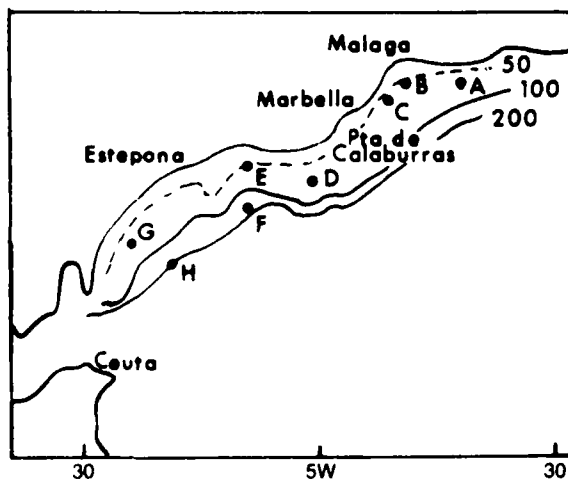


Figure 27. Locations of current meter moorings during 1978-1980.

that was formed when fresher water impinged on the Moroccan coast and later grew to become the big anti-cyclonic gyre (Whitehead and Miller, 1978). North of the Atlantic current several zones of cyclonic eddies have been detected (Lanoix, 1974; Cano, 1977, 1978a) beside the one already described above. In the western basin, near the Spanish coast between  $3^{\circ}$  and  $4^{\circ}$ W Lanoix (1974), as well as Cano (1977) and Parrilla (1983a, 1983b) (Fig. 25), noticed the presence of what seems to be a permanent cyclonic eddy. Cano (1978a) shows another weak cyclonic eddy northeast of the strait between Gibraltar and Malaga, where upwelling has been indicated (Fig. 14). Two surface drifters released near Gibraltar in October 1981 showed a cyclonic eddy near  $5^{\circ}$ W north of  $36^{\circ}$ N (C. Gascard, personal communication).

During 1978-1980 the Malaga Laboratory of the Instituto Español de Oceanografía deployed several current moorings for periods of one to two months along the Spanish coast (Fig. 27). From the results Arevalo and Garcia (1982) divided the area in two subregions. One was to the east of Punta de Calaburras ( $5^{\circ}$ W, Stations A,B,C), where the influence of the Atlantic current was weak, and another to the west, where the influence was stronger (Stations F and H). Stations D and E occupied an intermediate zone where the influence was intermittent; Station G seems to have been entirely sheltered from the Atlantic current.

Stations F and H were under the direct influence of the Atlantic inflow. Near the surface ( $\sim 20$  m) the mean direction was eastward at both sites and average speed was 20 cm/sec. The deep ( $\sim 100$  m) currents at H were southwestward and were opposite to the surface currents; the speed averaged 18 cm/sec. At F the deeper ( $\sim 80$  m) currents had two prevailing directions—NE and NW for more than 10 days each; average speeds were about 11 cm/sec. Stations D and E were intermittently subjected to the influence of the inflow, and the net results of the measured currents were eastward with average speeds smaller than 10 cm/sec. At Station G, a bimodal regime of directions parallel to the coast lasted two or three days each, and a weak lateral drift toward the coast. Mean speeds oscillated around 5 cm/sec. East of Punta de Calaburras all the stations had bimodal regimes. For B and C the directions were northeast and southwest with a coastward lateral drift at B. At A the main direction was east-northeast with westward fluctuations that lasted two or three days. The most important spectral characteristic was the influence of the semidiurnal tide, which was more intense to the west and slightly stronger at the surface. The contribution of the diurnal tides was similar to the semidiurnal, but less energetic.

Current meters were placed near  $4^{\circ}47'$ W on five moorings from  $36^{\circ}17'$ N to  $35^{\circ}58'$ N during June-October 1982 as part of the Donde Va experiment. Preliminary results showed mean velocities in the

Atlantic Water (defined by the 37.5 ppt isohaline) toward the east-northeast (041 to 062°T) at speeds from 9 to 53 cm/sec at depths from 62 to 124 m. All records showed a strong semidiurnal tidal oscillation, and significant fluctuations were present in the periods between 3 and 10 days.

## B. Mediterranean Water circulation

The circulation of the LIW and DW are not well known. Their mean velocities are small, probably 5–10 cm/sec for LIW and around 2 cm/sec for the DW. Ovchinnikov, depicting the geostrophic components of the currents at 500 dB relative to 1000 dB, described a cyclonic circulation below the anticyclonic gyre in the west Alboran Basin that coincided with a stronger signature of the LIW in the northern half of the basin and the southward veering of the isolines west of 3°W (Figs. 20 and 21). Bryden and Stommel (1982), on the other hand, calculated the geostrophic velocities and transports relative to the bottom for two vertical profiles across the western Alboran Sea. They suggested that the strongest maximum occurs where the flow of LIW is relatively slow and that this westward flow is stronger on the southern side, but that mixing with DW dilutes the properties of LIW on this side. May and Porter (1975) implied that this layer, as well as that of the deeper water, has the same vorticity as the surface layer in the zone of the anticyclonic gyre, so that the gyre can be interpreted as extending to the bottom.

As we have seen, the DW banks against the African coast, its isolines sloping upward, but not along, the Spanish coast. This water seems not to return eastward along the Spanish side, but to flow directly over the Gibraltar sill. Bryden and Stommel (1982) obtained an average flow of 4.6 cm/sec at 310°T from a 341-day current meter record obtained near the bottom of the African slope of the western Mediterranean Basin.

Recently, Pistek et al. (1982) studied the deep circulation using Swallow-type, acoustically tracked floats in the western Alboran. From January to May 1982, floats from 220 m to 1100 m revealed a broad and slow cyclonic circulation under the anticyclonic gyre. The average velocity was approximately 2 cm/sec. Part of the flow followed the bottom topography and, near the southern boundary, turned toward Gibraltar with velocities of 10 cm/sec; part turned eastward and followed the southern boundary of the deep channel toward Alboran Island.

During the Donde Va current meter deployment, three current meters were placed at 540-m depth from 36°17'N to 36°02'N along 4°47'N. These instruments were near the bottom of the intermediate water, above the 38.46 ppt isohaline. Means over the 112- to 114-day-long records varied from 235°T to 254°T, with speeds from 1.1 to 2.3 cm/sec. These flows point toward the Strait of Gibraltar, which suggests that the intermediate

water circulates cyclonically in the Alboran and that flow in the northern part of the Alboran may participate in the outflow. One deep instrument at a 910-m depth near 35°58'N had an eastward component of 0.1 cm/sec (the northward data channel failed). This supports the proposal of Bryden and Stommel (1982) that the major deep-water flow is in the southern part of the Alboran.

## VI. Tides and internal waves

Tides in the Alboran are a combination of the independent tide of the Mediterranean proper and of the passage of the North Atlantic tidal wave through the narrow Strait of Gibraltar. Because the Mediterranean is small and the strait is narrow, neither tide is large. The Atlantic tide causes appreciable tides in the Alboran near the strait, but they rapidly diminish eastward. Defant (1961) gave harmonic constants for several stations, and the largest constituents proceeding eastward illustrate this decrease: Cadiz, 93 cm ( $M_2$ ); Gibraltar, 38 cm ( $M_2$ ); and Alicante, 4 cm ( $K_1$ ).

Lacombe and Richez (1982) have studied the tide in the strait, where tidal currents exceeding 100 cm/sec are common. The tide in the strait acts against the strong stratification, and the sill forms large amplitude (> 100 m) peak-to-peak displacement in some cases) internal waves. In the strait the internal waves are modulated by the tides, but have periods of 10 to 40 min. Surface expressions have been detected both visually and by radar (Frassetto, 1964; Ziegenbein, 1969, 1970). Farther east, near 4°50'W close to the Spanish Coast, Lanoix (1974, Fig. 23) reported a single wave with a displacement near 100 m. We observed packets of such waves at five current meter moorings near the same longitude from 36°17'N to 35°58'N during June–October 1982. These waves were present at all depths from 67 to 910 m, and although they could be detected frequently at every current meter during every semidiurnal cycle, their strength was modulated at the diurnal frequency and also fluctuated on much longer time scales. It seems likely that the internal waves in the strait and the waves in the Alboran are manifestations of a solitary wave (or soliton) phenomenon forming at the sill and propagating eastward at 1–2 m/sec. Similar geophysical observations have been made in Knight Inlet (Farmer and Smith, 1980), the Strait of Messina (Alpers and Salusti, 1983), and in the Sulu Sea (Apel and Holbrook, 1983). This internal tidal wave may influence mixing across the pycnocline and tidal energy dissipation. It certainly poses sampling problems in the western Alboran.

## VII. Meteorological effects on the flow

Lacombe (1961), Crepon (1965), and Garrett (1983) discussed the probable influences of winds and atmospheric pressure on the AW inflow. When the average pressure over the Western Mediterranean is high, the sea surface is depressed and inflow decreases. When

pressure is low, the surface rises and AW inflow through the strait increases. Lacombe and Richez (1982) estimated that the inverted barometer effect could alter the inflow by one-fourth of its average for a 1-cm/day change in sea level over the entire Mediterranean. Garcia (1982), using time series of pressure and sea level at several locations, calculated the barometric factor at both sides of the strait; he found a high correlation between the pressure and the mean sea level at frequency bands of the passages of atmospheric systems (Gupta and Singh, 1977). He gives a table with some ratios between maximum, mean, and minimum inflow velocities. He found that in extreme conditions the inflow can change by a factor greater than 2.0, but for more typical conditions the inflow can change by a factor of 1.4. Westerly winds are associated with low pressures, which enhances the inflow. Lacombe and Tchernia (1972) suggested that this situation could increase the flow by a factor of 2.

Garrett (1983) recently resolved the paradox of both the sea level (rather than its time derivative) and the inflow being in phase with the (negative) atmospheric pressure (Crepon, 1965). Flow through the Strait of Sicily offers an adequate explanation, as perturbations about the mean sea levels in the western and eastern Mediterranean can be different over meteorologically important periods ( $\sim 10$  days). He further estimated that wind setup along the coast outside the strait is less important than atmospheric pressure fluctuations.

Cheney and Doblar (1982) showed an example of changes in the gyre that were possibly caused by atmospheric forcing. Three surveys were made in October 1977. Before the first survey the wind blew from the southwest at 5–13 m/sec, the pressure dropped 15 mbar and the gyre was located in its easternmost position. After this survey the wind shifted to the northeast and the pressure returned to 1020 mbar. The second survey 10 days later found the gyre at its westernmost position. The wind and pressure remained about the same until the third survey, as did the gyre position. In the same paper they showed a more dramatic case (reproduced from Kerling, 1977) in May 1977, when pressure dropped 10–15 mbar and a westerly wind blew at 18–25 m/sec. The AW vein exhibited little curvature; the gyre was very small and its center quite displaced to the south. They suggested that a slow initial speed at the strait generates a broad anticyclonic gyre in the western part of the Western Alboran Sea, while a faster current intrudes farther into the center of the western basin and pushes the gyre to the east.

Five days before the Alboran 80 cruise in April 1980 (Fig. 13) the pressure dropped 10 mbar below the average and remained so until the start of the survey and until the sea level at Ceuta and Tarifa rose about 20 cm. As can be seen, the vein is almost straight and reaches close to Alboran Island (Fig. 13), and the center of the gyre was situated in the south and displaced to

the east. This is similar to the Cheney and Doblar description, but the wind blew from the east for 15 days before the cruise, with gusts in the strait surpassing 20 m/sec. During the cruise the pressure rose to normal values ( $\sim 1020$  mbar) and the sea level dropped 20 cm; the wind was weak with variable direction from east and west. The fact that, in theory, opposite actions—the low pressure and the easterly wind—were taking place at the same time is perhaps what made a more complex picture at 30 m, where the influence of the wind is stronger than at 100 m.

After reviewing all these potential causes that influence the gyre, it seems that an important task is discerning to what degree the gyre variations are related to the temporal scales of the different influences. As Bucca and Kinder (1984) pointed out, short duration events—they referred to atmospheric forcing, but the idea may be applied to other forcing as well—can change the surface signature, which might not influence the gyre beneath it. The deeper gyre may respond only to influences of longer periods.

## VIII. The future

Several techniques hold promise for increasing the oceanographic understanding of the Alboran Sea. New instruments will allow better determinations of traditionally measured properties such as temperature, salinity, and velocity. Increased accuracy and better resolution in both space and time will lead to more precise definitions of the distributions and flows of the Atlantic and Mediterranean waters, and of the processes that cause them. Uniform calibration procedures for the range of temperature and salinity in the Mediterranean Water are needed for more meaningful comparisons between data sets and for the detection of climatological changes. Remote sensing, especially from satellite, will permit synoptic views of the upper layer and will both complement traditional measurements and contribute new insights of its own. Modeling the flow in the Alboran Sea, through either numerical or laboratory simulation, will increase our dynamical knowledge.

Many interesting research problems can be addressed in the Alboran Sea, and many of these problems are intimately linked to problems in the Strait of Gibraltar and the entire Mediterranean. Variations of the inflow at time scales from seasonal to tidal and their effect on the Alboran Gyre and the entire Mediterranean need elucidation. Meteorological effects are believed important, but this has not been proven. The kinematics and dynamics of the outflow and the relative contributions of different waters to the outflow are likewise unknown. The dynamics of the flow in the strait, the mixing between inflowing and outflowing waters, and the action of the strait as a control on the entire Mediterranean are problems that are fundamental to basic scientific understanding and to such practical

questions as pollution dispersion. Long-term fluctuations in the Mediterranean water (LIW and DW) may be an especially useful monitor on climatic changes in the Mediterranean. Several aspects of the internal wave packets are interesting, both fundamentally and locally: their generating mechanism, their spreading and dissipation, and their effect on the kinetic energy and mixing in the strait and in the Alboran Sea. There is presently active work on these and other problems using the techniques mentioned in the preceding paragraph. We hope that progress makes this overview of the Alboran Sea soon outdated.

## IX. Summary

Atlantic water, defined by salinities of less than 36.5 ppt, flows into the Alboran Sea through the Strait of Gibraltar at speeds exceeding 1 m/sec. This water flows eastward as a narrow (< 30 km) and shallow (< 200 m) vein, which forms a large anticyclonic gyre that typically dominates the western Alboran. Flow continues eastward, either north or south of Alboran Island, and forms large meanders and eddies in the eastern Alboran.

Below 200 m depth the basin is filled with Mediterranean water that is characterized by salinities exceeding 38.4 ppt. Between 200 and 600 m, a remnant of Levantine Intermediate Water ( $S \sim 38.47$  ppt and  $\theta \sim 13.15^\circ\text{C}$ ) flows westward, preferentially in the northern half, and forms a cyclonic circulation in the western Alboran Sea (opposite to the overlying Atlantic water circulation). This water contributes to the outflow through the strait, and recent measurements below the core of this water showed velocities of 1–2 cm/sec toward the strait. This water has shown substantial variations in temperature and salinity over the past 20 years, in part because of variations in the winter-formed temperature minimum layer above it. Below 600 m, the Deep Water flows westward, constrained by the topography to pass north of Alboran Island. Unlike the Intermediate Water, it hugs the African slope (the channel north of Alboran Island is oriented toward the south). Deep Water also contributes to the outflow, and velocities of 5 cm/sec toward the strait have been measured.

Tides are strong near the strait, but rapidly diminish eastward. Within the strait, however, tides generate internal waves, which may perturb both density and velocity fields far to the east.

Both wind stress and atmospheric pressure are believed important, perhaps in the mean upper layer flow, but certainly in fluctuations about the mean. Atmospheric forcing has been directly linked to sea level fluctuations, but such basic knowledge as the seasonal variation of inflow and outflow through the Strait of Gibraltar is lacking.

Research that will probably be conducted in the next five years should significantly broaden and deepen our knowledge of physical processes in the Alboran Sea.

## X. An update on related publications

Since original completion of this report in the fall of 1983, several important papers on the Alboran Sea have appeared. Many of these papers are contributions from the Donde Va project, which stimulated this report.

Boyle, E. A., S. D. Chapnick, X. X. Bai, and A. Spivak (1985). Trace metal enrichments in the Mediterranean Sea. *Earth and Planetary Science Letters* 74:405–419.

Describes a trace metal plume that was coincident with the inflowing Atlantic current.

Donde Va Group (1984). Donde Va? An oceanographic experiment in the Alboran Sea. *EOS* 65:682–683.

Describes the 1982 experiment and preliminary results.

Gascard, J. C. and C. Richez (1985). Water masses and circulation in the western Alboran Sea and in the Strait of Gibraltar. *Progress in Oceanography* 15:157–216.

Reports on French hydrographic and Lagrangian drifter measurements in the western Alboran Sea and in the Strait of Gibraltar.

Hogg, N. G. (1985). Multilayer hydraulic control with application to the Alboran Sea circulation. *Journal of Physical Oceanography* 15:454–466.

Formulates a theory of multiple-layer hydraulic control to explain some features of the Alboran Sea circulation.

Hsu, S. A., R. Fett, and P. E. La Violette (1985). Variations in atmospheric mixing height across oceanic thermal fronts. *Journal of Geophysical Research* 90:3211–3224.

Describes variations in the lower atmosphere across the front that marks the northern boundary of the inflowing Atlantic surface waters.

Janopaul, M. M. and A. S. Frisch (1984). CODAR measurements of surface currents in the northwestern Alboran Sea during the Donde Va experiment. *Annales Geophysicae* 2:443–448.

Describes shore-based radar measurements of surface currents near the Spanish coast.

Kinder, T. H. (1984). Net mass transport by internal waves near the Strait of Gibraltar. *Geophysical Research Letters* 11:987–990.

Reports on 16-week-long records of nonlinear internal wave packets propagating from the Strait of Gibraltar.

La Violette, P. E. (1985). The advection of submesoscale thermal features in the Alboran Sea gyre. *Journal of Physical Oceanography* 14:550–565.

Reports on recurring thermal surface features that are advected around the gyre.

La Violette, P. E. (1985). Short-term measurements of surface currents associated with the Alboran Sea during Donde Va. *Journal of Physical Oceanography* 16:262-279.

Reports on short-term current measurements in the gyre.

Parrilla, G., T. H. Kinder, and R. H. Preller (1985). Deep and intermediate water in the western Alboran Sea. *Deep-Sea Research* 33:55-88.

Uses hydrographic and direct current measurements and a numerical model to describe and explain the Mediterranean Water structure and flow in the Alboran Sea.

Pistek, P., F. de Strobel, and C. Montanari (1985). Deep sea circulation in the Alboran Sea. *Journal of Geophysical Research* 90:4969-4976.

Uses Lagrangian floats to describe the Mediterranean Water flow in the western Alboran.

Preller, R. H. (1985). A numerical model of the Alboran Sea gyre. *Progress in Oceanography* 16:113-146.

Elucidates the dynamics of the Alboran Sea gyre using a numerical model.

Whitehead, J. A. (1985). A laboratory study of gyres and uplift near the Strait of Gibraltar. *Journal of Geophysical Research* 90:7045-7060, and correction, 90:12,011-12,013.

Uses a rotating laboratory model to examine the effect of the gyre of the outflowing Mediterranean Water.

## XI. References

Admetlla, R. (1980). *Informe de vientos costeros el Mar de Alboran*. Unpublished manuscript.

Alpers, W. and E. Salusti (1983). Scylla and Charybdis observed from space. *Journal of Geophysical Research* 83(C3):1800-1808.

Anati, D. and H. Stommel (1970). The initial phases of deep-water formation in the Northwest Mediterranean during Medoc '69 on the basis of observations made by Atlantis II, January 25, 1969 to February 12, 1969. *Cahiers Oceanographiques* 22(4):343-351.

Anonymous (1982). Guia Resumida del Clima eu Espana. *Servicio de Climatologia*. Instituto Nacional de Meteorologia, Madrid, Spain, Publ. D-25, 52 pp.

Apel, J. R. and J. R. Holbrook (1983). The Sulu Sea internal soliton experiment. Submitted to *Journal of Physical Oceanography*.

Arevalo, L. and T. Garcia (1982). *Corrientes de la costa de Malaga, Metodos y resultados*. Inf. Tecn. del I.E.O., Madrid, Spain (in press).

Brody, L. R. and M. J. R. Nestor (1980). *Regional Forecasting Aids for the Mediterranean Basin*. Naval Environmental Prediction Research Facility, Monterey, California, Technical Report 80-10.

Bryden, H. L., R. C. Millard, and D. L. Porter (1978). *CTD Observations in the western Mediterranean Sea during Cruise 118, Leg 2 of R/V Chain, February, 1975*. Woods Hole Oceanographic Institution, Woods Hole, Massachusetts, Technical Report 78-26, March, 38 pp.

Bryden, H. L. and H. M. Stommel (1982). Origin of Mediterranean outflow. *Journal of Marine Research* 40(S):55-71.

Bucca, P. A. and T. H. Kinder (1984). An example of meteorological effects on the Alboran Sea Gyre. *Journal of Geophysical Research*, 89:751-757.

Bunker, A. F. (1972). Wintertime interactions of the atmosphere with the Mediterranean Sea. *Journal of Physical Oceanography* 2:225-238.

Burkov, V. A., V. G. Krivosheya, I. M. Ovchinnikov, and M. T. Savin (1979). Eddies in the current system of the western Mediterranean Basin. *Oceanology* 19(1):9-13.

Cano, N. (Lucaya) (1977). Resultados de la campana "Alboran 73." *Boletin del Instituto Español de Oceanografia*, Tomo I, Enero.

Cano, N. (Lucaya) (1978a). Resultados de la campana "Alboran 76." *Boletin del Instituto Español de Oceanografia*. No. 247:3-50.

Cano, N. (Lucaya) (1978b). Hidrologia del Mar de Alboran en primavera-verano. *Boletin del Instituto Español de Oceanografia*. No. 248:51-66.

Cano, N. (Lucaya) and F. Fernandez (1968). Variacion Estacional de la inclinacion transversal de las aguas atlanticas y Mediterraneas en el Estrecho de Gibraltar. *Boletin del Instituto Español de Oceanografia*. No. 136:23.

Cano, N. (Lucaya) and T. Gil (1982). Campana hidrologica Alboran 78. *Boletin del Instituto Español de Oceanografia* (In press).

Capart, J. I. and M. Steyaert (1963). *Mission O.T.A.N. en mer d'Alboran. Rapport preliminaire. Temperatures et courants de surface enregistres a bord du navire belge Eupen*. NATO Technical Report 9, Brussels.

Carter, D. B. (1956). The water balance of the Mediterranean and Black Seas. *Publications in Climatology* 9(3):123-174, Drexel Institute of Technology.

Carter, T. G., J. P. Flanagan, C. R. Jones, F. L. Marchant, R. R. Murchinson, J. H. Rebman, J. C. Sylvester, and J. C. Whitney (1972). A New Bathymetric Chart and Physiography of the Mediterranean Sea. In *The Mediterranean Sea: A Natural Sedimentation Laboratory*. D. J. Stanley, G. Kelling, and Y. Weiler (eds.), Dowden, Hutchinson, and Ross, Inc., Stroudsburg, Pennsylvania.

Cheney, R. E. and R. A. Doblar (1982). Structure and Variability of the Alboran Sea Frontal System. *Journal of Geophysical Research* 87(C1):585-594.

Copin-Montegut, G., B. Coste, J.-C. Gascard, J. Gostan, P. Le Corre, H. J. Minas, T. T. Packard,



and A. Poisson (1982). Nutrient regeneration and circulation patterns in the Strait of Gibraltar and in the Western Mediterranean Sea. *EOS* 63(3):109.

Crepon, M. (1965). Influence de la pression atmospherique sur le niveau moyen de la Mediterranee occidentale et sur le flux a travers le Detroit de Gibraltar. Presentation d'observations. *Cahiers Oceanographiques* 17(1):15-32.

Defant, A. (1961). *Physical Oceanography*, Vol. II, Pergamon.

Farmer, D. M. and J. D. Smith (1980). Tidal interaction of stratified flow with a sill in Knight Inlet. *Deep-Sea Research* 27:239-254.

Fenner, D. R. (1979). *Sound Speed and Oceanic Frontal Variability in the Western Alboran Sea (January-March 1979)*. Naval Ocean Research and Development Activity, NSTL, Mississippi, Technical Note 52, 35 pp.

Frassetto, R. (1964). *Short Period Vertical Displacements of the Upper Layers in the Straits of Gibraltar*. SACLANT ASW Research Centre, La Spezia, Italy, Technical Report 30, 49 pp.

Gallagher, J. J., M. Felcher, and J. Gorman (1981). *Project Huelva.-Oceanographic/Acoustic Investigation of the Western Alboran Sea*. Naval Underwater Systems Center, New London, Connecticut, Technical Report 6023, 106 pp.

Garcia, T. (1982). Barometric factor at both sides of the Strait of Gibraltar. Its relationship with inflow variations. *Rapp. CIESM* 28 (in press).

Garrett, C. (1983). Variable sea level and strait flows in the Mediterranean: A theoretical study of the response to meteorological forcing. *Oceanologica Acta* 6(1):79-87.

Garzoli, S. and C. Millard (1979). Winter circulation in the Sicily and Sardinia Straits region. *Deep-Sea Research* 26A:933-954.

Giermann, G. (1962). Erlauterungen zur bathymetrischen karte des westlichen Mittelmeers (zwischen 6°40'W.L. und 1°0'E.L.) *Bulletin de l'Institut Oceanographique* 1254:24 p.

Giermann, G., M. Pfannenstiel and W. Wimmenauer (1968). Relations entre morphologie, tectonique et volcanisme en mer d'Alboran (Mediterranee Occidentale). Resultats preliminaires de la campagne JEAN-CHARCOT (1967). *Comptes Rendus Sommaire de Seances de la Societe Geologique de France* 4:116-117.

Grousson, R. and J. Faroux (1963). Mesure de courants de surface en mer d'Alboran. *Cahiers Oceanographiques* 15:716-721.

Gupta, B. R. D. and B. Singh (1977). A power spectrum analysis of the mean daily pressure over the Mediterranean and neighbourhood during November 1967 to April 1968. *Tellus* 29:382-384.

Hopkins, T. S. (1978). Physical processes in Mediterranean Basins. In *Estuarine Transport Processes*, B. Kjerfve (ed.), University of South Carolina Press, Columbia, pp. 269-310.

Huang, T. C. and D. J. Stanley (1972). Western Alboran Sea: sediment disposal, ponding and reversal of currents. In *The Mediterranean Sea: A Sediment Laboratory*, Dowden, Hutchinson, and Ross, Stroudsburg, Pennsylvania, pp. 521-559.

Katz, E. J. (1972). The Levantine intermediate water between the Strait of Sicily and the Strait of Gibraltar. *Deep-Sea Research* 19:507-520.

Kerling, J. L. (1977). *Alboran Sea Temperature Survey*, preliminary report, data analysis. Unpublished report, 5 pp. plus 24 figs., plus appendix, U.S. Naval Oceanographic Office, NSTL, Mississippi.

Kinder, T. H., D. A. Burns, Z. R. Hallock, and M. J. Stirgus (1983). *Hydrographic Measurements in the Western Alboran Sea, June 1982, Donde Va?* Naval Ocean Research and Development Activity, NSTL, Mississippi, Technical Note 202, 127 pp.

Lacombe, H. (1961). Contribution a l'etude du regime de detroit de Gibraltar. I. Etude dynamique. *Cahiers Oceanographiques* 13(2):73-107.

Lacombe, H. (1974). Deep effects of energy transfers across the sea surface: the formation of deep waters. The Western Mediterranean as an example. Presid. IAPSO Melbourne Assembly, *IAPSO Proces-Verbaux* 13:52-85.

Lacombe, H., J. C. Gascard, J. Gonella, and J. P. Bethoux (1981). Response of the Mediterranean to the water and energy fluxes across its surface, on seasonal and interannual scales. *Oceanologica Acta* 4(2): 247-255.

Lacombe, H. and C. Richez (1982). The regime of the Strait of Gibraltar. In *Hydrodynamics of Semi-Enclosed Seas*, J. C. J. Nihoul (ed.), Elsevier, pp. 13-73.

Lacombe, H. and P. Tchernia (1960). Quelques traits generaux de l'hydrologie Mediterranee. *Cahiers Oceanographiques* 12(8):527-547.

Lacombe, H. and P. Tchernia (1972). Caracteres hydrologiques et circulation des eaux en Mediterranee. In *The Mediterranean Sea*, D. J. Stanley (ed.), Dowden, Hutchinson, and Ross, Stroudsburg, Pennsylvania, pp. 26-36.

Lanoix, F. (1974). *Projet Alboran, Etude hydrologique et dynamique de la mer d'Alboran*. North Atlantic Treaty Organization, Brussels, Technical Report 66.

La Violette, P. E. (1983). The advection of cyclic submesoscale thermal features in the Alboran Sea Gyre. Submitted to *Journal of Physical Oceanography*.

May, P. W. (1982). *Climatological Flux Estimates in the Mediterranean Sea: Part I. Winds and Wind Stress*. Naval Ocean Research and Development Activity, NSTL, Mississippi, Technical Report 54, 59 p.



- May, P. W. and D. L. Porter (1975). Geostrophic calculations for the Alboran Sea. *EOS* 56(6):377.
- Miller, A. R. (1982). Levantine Intermediate Water and its condition within the Alboran Sea. *Rapport CIESM* 28 (in press).
- Milliman, J. D., Y. Weiler, and D. J. Stanley (1972). Morphology and carbonate sedimentation on shallow banks in the Alboran Sea. In *The Mediterranean Sea. A Natural Sedimentation Laboratory*, D. J. Stanley, G. Kelling, and Y. Weiler (eds.), Dowden, Hutchinson, and Ross, Inc., pp. 241-259.
- Morcos, S. A. (1972). Sources of Mediterranean Intermediate water in the Levantine Sea. In *Studies in Physical Oceanography, Volume II*. Gordon and Breach, Scientific Publishers, New York, pp. 185-206.
- Nielsen, T. H. (1912). *Hydrography of the Mediterranean and adjacent waters*. Rap. Dan. Oceanogr. Exped. 1908-1910, I, 76, Copenhagen.
- Nof, D. 1978. On geostrophic adjustment in sea straits and wide estuaries: theory and laboratory experiments; Part II—Two layer system. *Journal of Physical Oceanography* 8(5):861-872.
- Ovchinnikov, I. M. (1966). Circulation in the surface and intermediate layers of the Mediterranean. *Oceanology* 6:48-59.
- Ovchinnikov, I. M. (1974). On the water balance of the Mediterranean Sea. *Oceanology* 14(2):25-255 (in Russian).
- Ovchinnikov, I. M. and Ye. A. Plakhin (1965). Formation of Mediterranean deep water masses. *Oceanology* 5(4):40-47.
- Ovchinnikov, I. M., V. G. Krivosheya, and L. V. Maskalenko (1976). Anomalous features of the water circulation of the Alboran Sea during Summer 1962. *Oceanology* 15:31-35.
- Parrilla, G. (1983a). Nota sobre el giro anticiclónico en el Mar de Alboran. IV Asamblea Nacional de Geodesia y Geofísica, *Comunicaciones* 3, Zaragoza: 1151-1166.
- Parrilla, G. (1983b). Mar de Alboran. Situación del giro anticiclónico en Abril de 1980. *Boletín del Instituto Español de Oceanografía* (in press).
- Parrilla, G. and T. Salat (1982). Atlantic Circulation in the Alboran Sea, Fall 1981. *Rapport CIESM* (in press).
- Peluchon, G. (1965). *Projet Alboran I: Resultats des observations oceanographiques effectues en Mer d'Alboran en Juillet-Aout 1962*. Techn. Report 26 et 27. Paris, December 1965.
- Philippe, M. (1980). Front Thermiques et Méditerranée d'après les données du radiomètre du satellite NOAA 5 (Septembre 1977-Février 1979). *C.R. Acad. Sc. Paris*, t. 2913 (1):43-46.
- Philippe, M. and L. Harang. (1982). Surface temperature fronts in the Mediterranean Sea from infrared satellite imagery. In *Hydrodynamics of Semi-enclosed Seas*, J. C. J. Nihoul (ed.), Elsevier, pp. 91-128.
- Pistek, P., F. D. Strobel, and C. Montanari (1982). Deep Sea Circulation in the Alboran Basin. *Rapport CIESM* 28, (in press).
- Preller, R. and H. E. Hurlburt (1982). A reduced gravity model of circulation in the Alboran Sea. In *Hydrodynamics of Semi-enclosed Seas*, J. C. J. Nihoul (ed.), Elsevier, pp. 75-90.
- Saint-Guilly, B. (1957). Les meandres des veines de courant dans les océans. *Bull. de l'Inst. Oceanographique* No. 1108.
- Sankey, T. (1973). The formation of deep water in the NW Mediterranean. *Progress in Oceanography* 6:159-179.
- Seco, E. (1959). La capa de velocidad cero en el mar de Alboran. *Revista Las Ciencias* XXV(4):765-779.
- Stevenson, R. E. (1977). Huelva front and Malaga, Spain, eddy chains as defined by satellite and oceanographic data. *Deut. Hydrogr. Z.* 30(2):51-53.
- Stommel, H. M., H. Bryden, and P. Manglesdorf (1973). Does some of the Mediterranean outflow come from great depth? *Pure Appl. Geophys.* 105:874-889.
- Sverdrup, H. V., M. W. Johnson, and R. H. Fleming (1942). *The Oceans*, Prentice-Hall, 1087 pp.
- Tchernia, P. (1960). Hydrologie d'hiver en Méditerranée Occidentale. *Cahiers Oceanographiques* 12:184-198.
- United Nations Environmental Program (1979). *Pollutants d'origine tellurique dans la Méditerranée*. W.G. 181 Inf. 4. GE79-2184.
- Wannamaker, B. (1979). *The Alboran Sea Gyre: Ship, Satellite and Historical Data*. SACLANT ASW Research Centre, La Spezia, Italy, Report SR-30, 15 June, 27 pp.
- Whitehead, J. A. and A. R. Miller (1979). Laboratory simulation of the gyre in the Alboran Sea. *Journal of Geophysical Research* 84(C7):3733-3742.
- Wust, G. (1960). Die Tiefenzirkulation des Mitteländischen Meeres in den Kernschichten des Zwischen und des Tiefenwasser. *Deuts. Hydrogr. Zeits.* 13(3): 105-131.
- Wust, G. (1961). On the vertical exchange of the Mediterranean Sea. *Journal of Geophysical Research* 66(10):3261-3271.
- Ziegenbein, J. (1970). Spatial observations of short internal waves in the Straits of Gibraltar. *Deep-Sea Research* 17(5):867-876.
- Ziegenbein, J. (1969). Short internal waves in the Straits of Gibraltar. *Deep-Sea Research* 16(5): 479-487.

UNCLASSIFIED

SECURITY CLASSIFICATION OF THIS PAGE

REPORT DOCUMENTATION PAGE																
1a. REPORT SECURITY CLASSIFICATION <b>Unclassified</b>		1b. RESTRICTIVE MARKINGS <b>None</b>														
2a. SECURITY CLASSIFICATION AUTHORITY		3. DISTRIBUTION/AVAILABILITY OF REPORT  <b>Approved for public release; distribution is unlimited.</b>														
2b. DECLASSIFICATION/DOWNGRADING SCHEDULE																
4. PERFORMING ORGANIZATION REPORT NUMBER(S)  <b>NORDA Report 184</b>		5. MONITORING ORGANIZATION REPORT NUMBER(S)  <b>NORDA Report 184</b>														
6. NAME OF PERFORMING ORGANIZATION  <b>Naval Ocean Research and Development Activity</b>		7a. NAME OF MONITORING ORGANIZATION  <b>Naval Ocean Research and Development Activity</b>														
8c. ADDRESS (City, State, and ZIP Code)  <b>Ocean Science Directorate NSTL, Mississippi 39529-5004</b>		7b. ADDRESS (City, State, and ZIP Code)  <b>Ocean Science Directorate NSTL, Mississippi 39529-5004</b>														
8a. NAME OF FUNDING/SPONSORING ORGANIZATION <b>Naval Ocean Research and Development Activity</b>		8b. OFFICE SYMBOL (If applicable)		9. PROCUREMENT INSTRUMENT IDENTIFICATION NUMBER												
8c. ADDRESS (City, State, and ZIP Code)  <b>Ocean Science Directorate NSTL, Mississippi 39529-5004</b>		10. SOURCE OF FUNDING NOS. <table border="1"><thead><tr><th>PROGRAM ELEMENT NO</th><th>PROJECT NO</th><th>TASK NO.</th><th>WORK UNIT NO</th></tr></thead><tbody><tr><td>61153N</td><td>03204</td><td>0D0</td><td>13317E</td></tr></tbody></table>			PROGRAM ELEMENT NO	PROJECT NO	TASK NO.	WORK UNIT NO	61153N	03204	0D0	13317E				
PROGRAM ELEMENT NO	PROJECT NO	TASK NO.	WORK UNIT NO													
61153N	03204	0D0	13317E													
11. TITLE (Include Security Classification) <b>The Physical Oceanography of the Alboran Sea</b>																
12. PERSONAL AUTHOR(S) <b>Gregorio Parrilla* and Thomas H. Kinder</b>																
13a. TYPE OF REPORT  <b>Final</b>		13b. TIME COVERED From _____ To _____		14. DATE OF REPORT (Yr., Mo., Day)  <b>March 1987</b>												
15. PAGE COUNT  <b>26</b>																
16. SUPPLEMENTARY NOTATION <b>Instituto Español de Oceanografía, Madrid, Spain</b>																
17. COSATI CODES <table border="1"><thead><tr><th>FIELD</th><th>GROUP</th><th>SUB. GR.</th></tr></thead><tbody><tr><td> </td><td> </td><td> </td></tr><tr><td> </td><td> </td><td> </td></tr><tr><td> </td><td> </td><td> </td></tr></tbody></table>			FIELD	GROUP	SUB. GR.										18. SUBJECT TERMS (Continue on reverse if necessary and identify by block number)  <b>Alboran Sea, Mediterranean Sea, meteorology water masses, circulation, waves</b>	
FIELD	GROUP	SUB. GR.														
19. ABSTRACT (Continue on reverse if necessary and identify by block number)  <p>The Alboran Sea is the westernmost basin of the Mediterranean Sea. Research published through 1983 is synthesized to show the important physical oceanographic features of the Alboran Sea. The upper layer of the Alboran Sea extends to about 200 m depth, and is characterized by low salinity (36 or less) and by an energetic anticyclonic gyre, whose speeds may exceed 1 m/sec and which may fill most of the western Alboran. Beneath the generally eastward-flowing Atlantic Water are two Mediterranean waters. The Levantine Intermediate Water, which extends from about 200 to 600 m depth, has maxima in both salinity (about 38.45) and temperature. The Levantine Water moves westward at 1-3 cm/sec in a broad flow that is concentrated in the northern part of the basin. Below the Levantine Water the Western Mediterranean Deep Water has steadily decreasing salinity and temperature to values below 12.9°C potential temperature, which has been taken as a definition. The deep-water flow is concentrated as a narrow boundary current against the African slope and has a speed of 5-10 cm/sec to the west.</p>																
20. DISTRIBUTION/AVAILABILITY OF ABSTRACT  UNCLASSIFIED/UNLIMITED <input type="checkbox"/> SAME AS RPT. <input checked="" type="checkbox"/> DTIC USERS <input type="checkbox"/>			21. ABSTRACT SECURITY CLASSIFICATION  <b>Unclassified</b>													
22a. NAME OF RESPONSIBLE INDIVIDUAL  <b>Thomas H. Kinder</b>			22b. TELEPHONE NUMBER (Include Area Code)  <b>(601) 688-5253</b>	22c. OFFICE SYMBOL  <b>Code 331</b>												

END

DATE

FILMED

MARCH

1988

DTIC